Figure 4 | Apigenin improves glucose tolerance in miR103 transgenic mice. (a), Expression levels of mature miR103, miR122, and miR185 in liver tissues of miR103 transgenic mice (miR103 Tg) were determined by Northern blotting. (b), Expression levels of mature miR103 and its precursor in liver tissues of miR10-transgenic mice treated with apigenin were determined by Northern blotting. Control (DMSO) or apigenin (40 mg/kg) was injected intraperitoneally daily for 14 days. Representative results from three independent mouse sets are shown. (c), Liver tissue homogenates from miR103 transgenic mice were separated using a phos-tag gel to determine the phosphorylation status of TRBP. Representative results from three independent mouse sets are shown. Full-length blot image is available in Supplementary Figure 5g. (d), Blood glucose levels were determined at random times or after 12 h fasting in control and miR103 transgenic (miR103 Tg) mice (n = 8 in each group). Data represent the means ± s.d. *, $p < 0.05$ (t-test). (e), (f), Glucose and pyruvate tolerance tests in control, miR103 transgenic (miR103 Tg), and miR103 transgenic with apigenin treatment (miR103 Tg + apigenin) mice (n = 6 in each group). Data represent the means ± s.d. *, $p < 0.05$ (t-test).

showed impaired glucose tolerance after an intraperitoneal glucose injection, apigenin treatment significantly suppressed these phenomena (Figure 4e). Similarly, while miR103 transgenic mice showed increased glucose production during an intraperitoneal pyruvate-tolerance test, apigenin treatment also suppressed these effects (Figure 4f). In addition, an increased number of small adipocytes and a decreased number of large adipocytes were observed in apigenin-treated miR103 transgenic mice (Supplementary Figure 3e and f). These results suggest that apigenin may have beneficial effects on pathological conditions in miR103 transgenic mice.

Discussion

In this study, we demonstrated that apigenin (4',5,7-trihydroxyflavone) has inhibitory effects on the maturation processes of a subset of miRNAs and subsequent miRNA function. These effects may be mediated through inhibition of TRBP phosphorylation, possibly through inhibition of Erk activation. These results suggest that apigenin may be utilized to improve miRNA-mediated pathogenic states, such as glucose tolerance, induced by the over-expression of miRNA103.

Bioactive substances, such as caffeine and polyphenols, have been reported to have pleiotropic physiological effects[3,20]. However, those phenomena are descriptive in most cases and the underlying mechanisms are largely unclear. Apigenin, which is present in many fruits and vegetables, also has diverse biological effects, including improvement of the cancer cell response to chemotherapy[21], tumorigenesis[13,22], modulating immune cell function[23], and anti-platelet activity[24]. In this study, we showed that apigenin inhibits TRBP phosphorylation and its related miRNA maturation through inhibition of MAPK Erk activation. This modulation of miRNA function

by apigenin may account, at least in part, for its various reported biological effects.

Phosphorylation of TRBP is mediated by Erk[15]. We showed clear inhibition of Erk phosphorylation by apigenin. Although previous studies have reported the inhibition of Erk activation by apigenin[16-19], the underlying mechanisms were unknown. Because Erk has many biological functions in intracellular signaling, modulation of TRBP phosphorylation and miRNA expression induced by Erk inhibition through apigenin is likely a part of the phenotype. To clarify the biological function of apigenin, identification of molecules on which apigenin directly acts must be the next step.

Another important finding in this study was the impaired glucose tolerance observed in miR103 transgenic mice. Previous studies showed that recombinant adenoviruses expressing the miR103/ 107 family (only one nucleotide difference in miR103 and miR107 at position 21) and a gain of miR103/107 function by transient infection in mice was sufficient to induce impaired glucose homeostasis, and these miRNAs play a central role in insulin sensitivity[10]. In this study, we confirmed that constitutive expression of miR103 in mice resulted in impaired glucose tolerance and increased size of adipocytes. These mice may represent a new *in vivo* model of metabolic disorders and facilitate development of new drugs targeting impaired glucose tolerance. In fact, we found that apigenin reversed impaired glucose tolerance in miR103-transgenic mice. Because apigenin is one of the flavonoids and is present in high content in celery and parsley, intake of apigenin from foods or dietary supplements may have some favorable effects on glucose intolerance induced by overexpression of miRNA levels, even if it does not completely overcome impaired glucose tolerance.

Phosphorylated TRBP is not related to the maturation of all miRNAs, but rather a subset of miRNAs[15]. With this respect, apigenin may have favorable effects on the pathogenic status induced by overexpression or overfunction of the miRNAs to which phosphorylated TRBP is related. Maturation of miR122, a liver-specific miRNA, is at least partly regulated by apigenin, as shown in our study, its crucial function in cholesterol synthesis[11,25–28], and hepatitis c viral replication[29,30]. Therefore, apigenin may also have beneficial effects on these conditions. Other effects of apigenin on the pathological state may be necessary to reconsider from the point of view of overexpression or overfunction of specific miRNAs.

Simultaneously, one should be cautious about the modulation of miRNA function by apigenin. Because some miRNAs may have favorable effects on human health, apigenin might be harmful if it inhibits the maturation and function of such miRNAs. For example, inhibitory effects on tumor-suppressive miRNAs should be avoided. Caution regarding these issues is necessary and, in parallel, the biological functions of miRNAs in general should be further examined.

In summary, we showed that apigenin displays inhibitory effects on the phosphorylation of TRBP and its subsequent miRNA maturation and function through regulation of Erk activity. Decreasing miRNA function may be used for treatment of conditions induced by over-functioning of miRNAs. Moreover, clarifying the as-yet-undiscovered functions of bioactive substances is important. Similar strategies to those used here may also be applied to other bioactive substances whose effects have been reported but the mechanisms are as yet undetermined.

Methods

Cell culture. The human hepatocellular carcinoma cell lines, Huh7 and Hep3B, were obtained from the Japanese Collection of Research Bioresources (JCRB, Osaka, Japan). All cells were maintained in Dulbecco's modified Eagle's medium supplemented with 10% fetal bovine serum.

Reagents. Caffeine, apigenin and chlorogenic acid were purchased from Wako Chemicals (Osaka, Japan). Procyanidin A2 and B2 were purchased from Indofine Chemical (Hillsborough, NJ) and ChromaDex (Irvine, CA). Caffeine, chlorogenic acid and procyanidin B2 were dissolved in water. Apigenin and procyanidin A2 were dissolved in dimethyl sulfoxide (DMSO). Caffeine, chlorogenic acid and procyanidin A2 and B2 were added at concentrations of 20 µM, 10 µM, 50 µg/mL, and 50 µg/mL, respectively, as reported previously[11–31]. Apigenin was used at 10 µM unless otherwise specified for *in vitro* studies, and 40 mg/kg was used for intraperitoneal injection daily for *in vivo* studies. An equal volume of DMSO only was used as a negative control.

Mouse experiments. Experimental protocols were approved by the Ethics Committee for Animal Experimentation at the Graduate School of Medicine, the University of Tokyo and the Institute for Adult Disease, Asahi Life Foundation, Japan and conducted in accordance with the Guidelines for the Care and Use of Laboratory Animals of the Department of Medicine, the University of Tokyo, and the Institute for Adult Disease, Asahi Life Foundation.

Plasmids, transfection and dual luciferase assays. Plasmids expressing miR122 and miR185 precursors and the corresponding firefly luciferase-based reporters have been described previously[8,15]. Plasmids expressing miRNA-103 precursors and the corresponding luciferase reporter were newly constructed according to protocols reported previously[8]. To determine MAPK pathway activity, SRE-driven luciferase was transfected, and dual luciferase assays were performed as described previously[9], with the exception that pGL4.74, a control plasmid containing *Renilla reniformis* (sea pansy) luciferase under control of the herpes simplex virus thymidine kinase promoter (Promega), was used as an internal control. Chemicals were added at 24 h and the reporter assays were done 48 h post-transfection. Constitutively active MEK1(DD) and dominant negative Erk(K/N) constructs with zeocin resistance genes were kindly provided by Prof. Takekawa (The Institute of Medical Sciences, the University of Tokyo)[36]. After transfection, the cells were selected with 6 µg/mL zeocin to establish cells stably expressing those constructs.

Western blot analysis. Protein lysates were prepared from cells or mouse liver tissues for immunoblotting analyses. Western blotting was performed as described previously[8]. Primary antibodies were purchased from Sigma (DGCR8, #SAB4200088; Dicer, #SAB4200087; TRBP2, #SAB4200111; β-actin, #A5441), Bethyl (KSRP, A302-021), Wako (Ago2, 015-22031), and Cell Signaling (Drosha, #D28B1; Phospho-Erk, #9101; Total Erk, #4695; myc-tag, #2276; Caveolin, #3267).

Northern blotting of miRNAs. Northern blotting of miRNAs was performed as described previously[9]. Briefly, total RNA was extracted using TRIzol Reagent

(Invitrogen, Carlsbad, CA) according to the manufacturer's instructions. Ten micrograms of RNA were resolved in denaturing 15% polyacrylamide gels containing 7 M urea in 1× TBE and then transferred to a Hybond N+ membrane (GE Healthcare) in 0.25× TBE. Membranes were UV-crosslinked and prehybridized in hybridization buffer. Hybridization was performed overnight at 42°C in ULTRAhyb-Oligo Buffer (Ambion) containing a biotinylated probe specific for miR122 (CAA ACA CCA TTG TCA CAC TCC A), miR103 (TCA TAG CCC TGT ACA ATG CTG CT), miR185 (TCA GGA ACT GCC TTT CTC TCC A), and let-7g (AAC TGT ACA AAC TAC TAC CTC A), which had been heated to 95°C for 2 min. Membranes were washed at 42°C in 2× SSC containing 0.1% SDS, and the bound probe was visualized using a BrightStar BioDetect Kit (Ambion). Blots were stripped by boiling in a solution containing 0.1% SDS and 5 mM EDTA for 10 min prior to rehybridization with a U6 probe (CAC GAA TTT GCG TGT CAT CCT T).

Quantitative RT-PCR analysis of miRNA expression. To determine miR122, miR103, miR185, and let-7g expression levels, cDNA was first synthesized from RNA, and quantitative PCR was then performed using Mir-X miRNA First-Strand Synthesis and SYBR qRT-PCR Kit (Clontech). The expression levels of miRNA precursor were determined according to the previous report[17] using the reported primers. Relative expression values were calculated by the CT-based calibrated standard curve method. These calculated values were then normalized to the expression of U6 snRNA. The reverse primer was provided in the kit.

Determining TRBP phosphorylation status. Plasmids expressing wild-type TRBP and kinase-dead TRBP (TRBP SΔA) were kindly provided by Professor Liu[15]. Twenty-four hours after transfection into Huh7 cells with corresponding plasmids, substances were treated for 24 h, and cell lysates were collected for subsequent Western blotting. To better discriminate the phosphorylated form of TRBP from the unphosphorylated form, a Mn2+-Phos-tag SDS-PAGE gel (Wako) was used according to the manufacturer's instructions.

Generation of miR103-expressing transgenic mice. To construct transgenic mice, plasmids expressing miRNA-103 precursors were modified as follows: to add the SV40 poly(A) tail signal downstream of the miR103 precursor sequences, the pCDH-miR103 precursor-expressing plasmid was digested at the *NotI* restriction site, and PCR-amplified poly(A) tail signal sequences were digested with *ClaI* from the original plasmid as a template was inserted by the Infusion cloning system (Clontech, Mountain View, CA). A DNA fragment of 1,125 bp, containing the CMV promoter region, the 470-bp genomic region for the miR103 precursor, and a SV40 poly(A) tail signal, was resected from the constructed plasmid by digestion with *ClaI*. Stable C57BL/6 embryonic stem (ES) cell lines were generated by electroporation of the linearized transgene, and the resulting cells were injected into blastocysts by the UNITECH Company (Chiba, Japan). Genotyping was performed by PCR using DNA isolated from tail snips. Four different mouse lines were maintained and the male littermates were used in the experiments.

Glucose test. Blood glucose was tested using a Glucose Pilot system (Iwai Chemical, Japan). Glucose tolerance and pyruvate tolerance tests were performed by intraperitoneal injection of glucose (2 g/kg) or pyruvate (2 g/kg) after fasting overnight. Blood glucose levels were measured before injection (0 min) and at 15, 30, 60, and 120 min after injection.

Adipocyte size. Visceral fat tissues stained with hematoxylin and eosin were analyzed using the Image-J software. One hundred adipocytes were measured per animal to determine adipocyte size. The high-fat diet was purchased from CLEA-Japan (Tokyo, Japan).

miRNA microarray analyses. miRNA microarray analysis was performed using miRNA oligo chips (Toray Industries, Tokyo, Japan). Normalization was performed using the intensities from U6, instead of the standard global normalization. The data and the protocols were deposited in a public database (Please refer the following link during the review process; http://www.ncbi.nlm.nih.gov/geo/query/acc.cgi?token=frwpxomkicoicte&acc=GSE46526).

Statistical analysis. Statistically significant differences between groups were determined using Student's *t*-test when variances were equal. When variances were unequal, Welch's *t*-test was used. *P*-values less than 0.05 were considered to indicate statistical significance.

1. Surh, Y. J. Cancer chemoprevention with dietary phytochemicals. *Nat Rev Cancer* **3**, 768–780 (2003).
2. D'Incalci, M., Steward, W. P. & Gescher, A. J. Use of cancer chemopreventive phytochemicals as antineoplastic agents. *Lancet Oncol* **6**, 899–904 (2005).
3. Baur, J. A. *et al.* Resveratrol improves health and survival of mice on a high-calorie diet. *Nature* **444**, 337–342 (2006).
4. Carrington, J. & Ambros, V. Role of microRNAs in plant and animal development. *Science* **301**, 336–338 (2003).
5. Bartel, D. P. MicroRNAs: genomics, biogenesis, mechanism, and function. *Cell* **116**, 281–297 (2004).
6. Ambros, V. The functions of animal microRNAs. *Nature* **431**, 350–355 (2004).

7. Lu, J. *et al.* MicroRNA expression profiles classify human cancers. *Nature* **435**, 834–838 (2005).
8. Kojima, K. *et al.* MicroRNA122 is a key regulator of α-fetoprotein expression and influences the aggressiveness of hepatocellular carcinoma. *Nat Commun* **2**, 338 (2011).
9. Takata, A. *et al.* MicroRNA-140 acts as a liver tumor suppressor by controlling NF-κB activity by directly targeting DNA methyltransferase 1 (Dnmt1) expression. *Hepatology* **57**, 162–170 (2013).
10. Trajkovski, M. *et al.* MicroRNAs 103 and 107 regulate insulin sensitivity. *Nature* **474**, 649–653 (2011).
11. Krützfeldt, J. *et al.* Silencing of microRNAs in vivo with 'antagomirs'. *Nature* **438**, 685–689 (2005).
12. Budhraja, A. *et al.* Apigenin induces apoptosis in human leukemia cells and exhibits anti-leukemic activity in vivo. *Mol Cancer Ther* **11**, 132–142 (2012).
13. Shukla, S. *et al.* Blockade of beta-catenin signaling by plant flavonoid apigenin suppresses prostate carcinogenesis in TRAMP mice. *Cancer Res* **67**, 6925–6935 (2007).
14. Wang, W. *et al.* Cell-cycle arrest at G2/M and growth inhibition by apigenin in human colon carcinoma cell lines. *Mol Carcinog* **28**, 102–110 (2000).
15. Paroo, Z., Ye, X., Chen, S. & Liu, Q. Phosphorylation of the human microRNA-generating complex mediates MAPK/Erk signaling. *Cell* **139**, 112–122 (2009).
16. Yi Lau, G. T. & Leung, L. K. The dietary flavonoid apigenin blocks phorbol 12-myristate 13-acetate-induced COX-2 transcriptional activity in breast cell lines. *Food Chem Toxicol* **48**, 3022–3027 (2010).
17. Tatsuta, A. *et al.* Suppression by apigenin of peritoneal metastasis of intestinal adenocarcinomas induced by azoxymethane in Wistar rats. *Clin Exp Metastasis* **18**, 657–662 (2000).
18. Yin, F., Giuliano, A. E. & Van Herle, A. J. Signal pathways involved in apigenin inhibition of growth and induction of apoptosis of human anaplastic thyroid cancer cells (ARO). *Anticancer Res* **19**, 4297–4303 (1999).
19. Kuo, M. L. & Yang, N. C. Reversion of v-H-ras-transformed NIH 3T3 cells by apigenin through inhibiting mitogen activated protein kinase and its downstream oncogenes. *Biochem Biophys Res Commun* **212**, 767–775 (1995).
20. Yao, S. L. *et al.* Selective radiosensitization of p53-deficient cells by caffeine-mediated activation of p34cdc2 kinase. *Nat Med* **2**, 1140–1143 (1996).
21. Chan, L. P. *et al.* Apigenin induces apoptosis via tumor necrosis factor receptor- and Bcl-2-mediated pathway and enhances susceptibility of head and neck squamous cell carcinoma to 5-fluorouracil and cisplatin. *Biochim Biophys Acta* **1820**, 1081–1091 (2012).
22. Mafuvadze, B., Liang, Y., Besch-Williford, C., Zhang, X. & Hyder, S. M. Apigenin induces apoptosis and blocks growth of medroxyprogesterone acetate-dependent BT-474 xenograft tumors. *Horm Cancer* **3**, 160–171 (2012).
23. Nicholas, C. *et al.* Apigenin blocks lipopolysaccharide-induced lethality in vivo and proinflammatory cytokines expression by inactivating NF-kappaB through the suppression of p65 phosphorylation. *J Immunol* **179**, 7121–7127 (2007).
24. Landolfi, R., Mower, R. L. & Steiner, M. Modification of platelet function and arachidonic acid metabolism by bioflavonoids. Structure-activity relations. *Biochem Pharmacol* **33**, 1525–1530 (1984).
25. Hsu, S. H. *et al.* Essential metabolic, anti-inflammatory, and anti-tumorigenic functions of miR-122 in liver. *J Clin Invest* **122**, 2871–2883 (2012).
26. Lanford, R. E. *et al.* Therapeutic silencing of microRNA-122 in primates with chronic hepatitis C virus infection. *Science* **327**, 198–201 (2010).
27. Elmén, J. *et al.* LNA-mediated microRNA silencing in non-human primates. *Nature* **452**, 896–899 (2008).
28. Esau, C. *et al.* miR-122 regulation of lipid metabolism revealed by in vivo antisense targeting. *Cell Metab* **3**, 87–98 (2006).
29. Jopling, C. L., Yi, M., Lancaster, A. M., Lemon, S. M. & Sarnow, P. Modulation of hepatitis C virus RNA abundance by a liver-specific MicroRNA. *Science* **309**, 1577–1581 (2005).
30. Lindow, M. & Kauppinen, S. Discovering the first microRNA-targeted drug. *J Cell Biol* **199**, 407–412 (2012).
31. Ku, B. M. *et al.* Caffeine inhibits cell proliferation and regulates PKA/GSK3β pathways in U87MG human glioma cells. *Mol Cells* **31**, 275–279 (2011).
32. Nishizuka, T. *et al.* Procyanidins are potent inhibitors of LOX-1: a new player in the French Paradox. *Proc Jpn Acad Ser B Phys Biol Sci* **87**, 104–113 (2011).
33. Teraoka, M. *et al.* Cytoprotective effect of chlorogenic acid against α-synuclein-related toxicity in catecholaminergic PC12 cells. *J Clin Biochem Nutr* **51**, 122–127 (2012).
34. Shukla, S. & Gupta, S. Apigenin: a promising molecule for cancer prevention. *Pharm Res* **27**, 962–978 (2010).
35. Takata, A. *et al.* MicroRNA-22 and microRNA-140 suppress NF-κB activity by regulating the expression of NF-κB coactivators. *Biochem Biophys Res Commun* **411**, 826–831 (2011).
36. Kubota, Y., O'Grady, P., Saito, H. & Takekawa, M. Oncogenic Ras abrogates MEK SUMOylation that suppresses the ERK pathway and cell transformation. *Nat Cell Biol* **13**, 282–291 (2011).
37. Suzuki, H. I. *et al.* Modulation of microRNA processing by p53. *Nature* **460**, 529–533 (2009).

Acknowledgments

Author contributions

M.Ohno, C.S. and M.Otsuka planned the research and wrote the paper. M.Ohno, C.S., T.K., T.Y., A.T., K.Kojima, and M.Otsuka performed the majority of the experiments. M.A. and H.Y. contributed materials. Y.K. supported several experiments. K.Koike supervised the entire project.

Additional information

182

Original Article

Fibrosis score consisting of four serum markers successfully predicts pathological fibrotic stages of chronic hepatitis B

Kenji Ikeda,[1,2] Namiki Izumi,[3] Eiji Tanaka,[7] Hiroshi Yotsuyanagi,[4] Yoshihisa Takahashi,[5] Junichi Fukushima,[6] Fukuo Kondo,[5] Toshio Fukusato,[5] Kazuhiko Koike,[4] Norio Hayashi[8] and Hiromitsu Kumada[1,2]

[1]Department of Hepatology, Toranomon Hospital, [2]Okinaka Memorial Institute for Medical Research, [3]Department of Gastroenterology, Musashino Red Cross Hospital, [4]Department of Gastroenterology, Tokyo University of Medicine,[5]Department of Pathology, Teikyo University School of Medicine, [6]Department of Pathology, NTT Medical Center Tokyo, Tokyo, [7]Department of Gastroenterology, Shinshu University of Medicine, Matsumoto, and [8]Department of Gastroenterology, Kansai-Rosai Hospital, Hyogo, Japan

Aim: In order to evaluate and judge a fibrotic stage of patients with chronic hepatitis B, multivariate regression analysis was performed using multiple fibrosis markers.

Method: A total of 227 patients from seven hepatology units and institutes were diagnosed by needle biopsy as having chronic liver disease caused by hepatitis B virus. Twenty-three variables and their natural logarithmic transformation were employed in the multivariate analysis. Multiple regression function was generated from data of 158 patients in one hospital, and validation was performed using the other data of 69 patients from six other hospitals.

Results: After stepwise variable selection, multivariate regression analysis finally obtained the following function: $z = 1.40 \times \ln$ (type IV collagen 7S) (ng/mL) $- 0.017 \times$ (platelet count) ($\times 1000^3/mm^3$) $+ 1.24 \times \ln$ (tissue inhibitor of matrix metalloproteinase-2) (ng/mL) $+ 1.19 \times \ln$ (α-2-macroglobulin)

(mg/dL) $- 9.15$. Median values of fibrosis scores of F1 ($n = 73$), F2 ($n = 42$), F3 ($n = 31$) and F4 stages ($n = 12$) were calculated as 0.95, 2.07, 2.98 and 3.63, respectively. Multiple regression coefficient and coefficient of determination were *0.646* and *0.418*, respectively. Validation with patient data from other institutions demonstrated good reproducibility of fibrosis score for hepatitis B (FSB), showing 1.33 in F1 ($n = 27$), 2.20 in F2 ($n = 20$), 3.11 in F3 ($n = 20$) and 5.30 in F4 ($n = 2$), respectively.

Conclusion: A concise multiple regression function using four laboratory parameters successfully predicted pathological fibrosis stage of patients with hepatitis B virus infection.

Key words: chronic hepatitis, hepatitis B virus, liver cirrhosis, liver fibrosis, multiple regression analysis, stage

INTRODUCTION

WHEN HEPATITIS B virus (HBV)-related chronic liver disease is found by biochemical and virological examination, liver biopsy can establish the definitive diagnosis of chronic hepatitis and its fibrotic staging. Although these pathological procedures are reliable and informative both in diagnosis and treatment,

Correspondence: Dr Kenji Ikeda, Department of Hepatology, Toranomon Hospital, 2-2-2 Toranomon, Minato-ku, Tokyo, 105-8470, Japan. Email: ikedakenji@tora.email.ne.jp

they sometimes require medical invasion and financial costs, including the risk of bleeding from needle puncture, some pain experienced during the procedure and hospital stays of a few days. The pathological examination is, therefore, rarely performed repeatedly in a short period of time, unless disease activity is severe or progression of liver disease is highly suspected. Recently, many authors described the usefulness of ultrasonographic elastography and multiple resonance imaging technology in the estimation of staging of chronic hepatitis and cirrhosis.[1-5] These ways of estimation using the imaging apparatuses seem truly useful for current patients, but they cannot evaluate and compare with past fibrotic states of patients retrospectively. Moreover,

596

the same apparatus for elastometry will not be available for repeated measurement for a follow-up examination, for example, several years later.

In spite of the accuracy of biopsy and convenience of elastography in chronic liver disease, clinical diagnosis based on biochemistry and hematology is still indispensable for the daily practice of many patients with HBV-related liver disease. Recently, several studies were published about estimation of hepatitis stages, using one or more serum biomarkers. Discriminant functions or multivariate analyses demonstrated that approximately 60–90% of patients with chronic hepatitis B were correctly classified as having mild hepatitis and severe hepatitis with advanced fibrosis.[2,6–13] Up to the present time, however, the usefulness of the discriminant functions are less valuable for a few reasons. First, these functions were made for the purpose of discrimination of severe hepatic fibrosis from mild fibrosis, and four histological classifications (F1–F4) were neglected in almost of the studies. Second, some studies analyzed both hepatitis B and hepatitis C virus infection, although the significance and actual values of each liver function test in the evaluation of the severity of liver disease were not similar among each viral hepatitis and alcoholic liver disease. Third, biochemical markers for liver fibrosis (e.g. hyaluronic acid, type IV collagen, procollagen III peptide)[14–16] were not always included in those previous studies.

We tried to generate a function estimating fibrotic stages of HBV-related chronic hepatitis, which were objectively diagnosed by liver biopsy. The purpose of this study is, therefore, to make a reliable multiple regression function and to obtain practical coefficients for significant variables also using fibrosis markers.

METHODS

Patients

A TOTAL OF 273 Japanese patients with chronic hepatitis B were recruited for the study from seven hospitals in Japan: Toranomon Hospital, Hiroshima University Hospital (K. Chayama, M.D.), Ehime University Hospital (M. Onji, M.D.), Musashino Red Cross Hospital (N. Izumi, MD), Shishu University Hospital (E. Tanaka, M.D.), Showa University Hospital (M. Imawari, M.D.) and Osaka University Hospital (T. Takehara, M.D.). Inclusion criteria for this study were: (i) positive hepatitis B surface antigen for more than 6 months; (ii) persistent or intermittent elevation in aspartate aminotransferase (AST)/alanine aminotransferase (ALT) levels; and (iii) liver biopsy showing chronic hepatitis

(F1–F4). We excluded those patients with overt alcoholic liver disease or fatty liver, association of other types of liver disease (e.g. hepatitis C, primary biliary cirrhosis, autoimmune hepatitis), or those associated with hepatocellular carcinoma or other malignancy. Among the patients, 244 patients fulfilled the conditions for the study: complete demographic data, basic laboratory data of hematology and biochemistry, required liver biopsy specimens, and sufficient amount of frozen sera. Also, we excluded additional 17 patients with eventual histological diagnosis as F0 stage.

Finally, a total of 227 patients who were diagnosed as having chronic hepatitis or cirrhosis (F1–F4) were analyzed for the following hematological, biochemical and histopathological examination. There were 172 males and 55 females aged 16–70 years (median, 39 years).

All the patients presented written informed consent in individual hospitals and medical centers, and the study was approved in each ethical committee.

Hematological and biochemical examination

Hematological and standard biochemical evaluation had been performed in each medical institution: white blood cells, red blood cells, hemoglobin, platelets, total bilirubin, AST, ALT, AST/ALT ratio (AAR), γ-glutamyl transpeptidase (γ-GTP), total protein, albumin and γ-globulin.

Special biochemical examinations including "fibrosis markers" were carried out using stored frozen sera at $-20°C$ or lower: α-2-macroglobulin, haptoglobin concentration, haptoglobin typing, apolipoprotein A1, hyaluronic acid, tissue inhibitor of matrix metalloproteinase (TIMP)-1, TIMP-2, procollagen III peptide and type IV collagen 7S.

Histological diagnosis of chronic hepatitis and cirrhosis

All the 227 cases fulfilled required standards of histological evaluation: sufficient length of specimen, hematoxylin–eosin staining, and at least one specimen with fiber staining. Four independent pathologists (Y. T., J. F., F. K. and T. F.), who were not informed of patients' background and laboratory features except for age and sex, evaluated the 227 specimens regarding the stages of fibrosis and activity. Pathological classification of chronic hepatitis staging was based on Desmet *et al.*[17]

Before judgment of histological staging of individual specimens, the pathologists discussed the objective and reproducible judgment of pathological diagnosis of

hepatitis. They made a panel about obvious criteria using typical microscopic pictures for each stage, and it was always referred to during the procedure of pathological judgment. When inconsistent results were found in the diagnosis of hepatitis stage among the pathologists, the final judgment accepted majority rule among them.

Statistical analysis

Non-parametric procedures were employed for the analysis of background characteristics and laboratory data among patients in each stage, including Mann–Whitney U-test, Kruskal–Wallis test and χ^2-test.

The normality of the distribution of the data was evaluated by a Kolmogorov–Smirnov one-sample test. Because certain variables partly did not conform to a normal distribution, natural logarithmic transformation of bilirubin, AST, ALT, γ-GTP, α-2-macroglobulin, hyaluronic acid, type IV collagen 7S and TIMP-2 were also analyzed in the following calculation. The natural logarithmic transformation of the results yielded a normal distribution or symmetrical distribution for all the analyzed factors. After the procedures, the following multiple regression analysis became rationally robust against deviations from normal distribution. In order to avoid introducing into the model any variables that were mutually correlated, we checked the interaction between all pairs of the variables by calculating variance inflation factors. Of the highly correlated variables, less significant factors were removed from the viewpoint of multicollinearity.

Multivariate regression analysis was performed using 158 patient data from Toranomon Hospital (training dataset) to generate a training data of predicting function. We used a stepwise method for selection of informative subsets of explanatory variables in the model. Multiple regression coefficient and coefficient of determination were also taken into account in the selection of variables. Next, we validated the obtained predictive function using the remaining 69 patient data from the other six liver institutions (validation dataset).

A P-value of less than 0.05 with two-tailed test was considered to be significant. Data analysis was performed using the computer program SPSS ver. 19.[18]

For evaluation of the efficiency and usefulness of obtained function for fibrosis estimation, we compared various fibrosis scores for hepatitis B and C, including AAR,[19] AST-to-platelet ratio index (APRI),[20] FIB-4,[21] FibroTest[22] and discrimination function of cirrhosis from hepatitis in Japanese patients.[23]

RESULTS

Pathological diagnosis

FOUR PATHOLOGISTS INDEPENDENTLY judged the fibrotic stages and inflammatory activity for 227 specimens of chronic hepatitis/cirrhosis caused by HBV. One hundred patients (44.1%) had a fibrosis stage of F1, 62 (27.3%) F2, 51 (22.5%) F3 and 14 (6.2%) F4. In the subgroup of the 158 patients in the training group, judgment as F1 was made in 73 cases, F2 in 42, F3 in 31 and F4 in 12. Of the 69 patients in the validation group, judgment as F1 was made in 27, F2 in 20, F3 in 20 and F4 in two.

According to hepatitis activity classification, A0 was found in five (2.2%), A1 in 100 (44.1%), A2 in 107 (47.1%) and A3 in 15 (6.6%).

Laboratory data of each hepatitis stage in the training group

There were 124 men and 34 women with a median age of 39 years ranged 16–70 years. Laboratory data of 158 patients in the training group are shown in Table 1. Although several individual items were well correlated with the severity of hepatic fibrosis, significant overlap values were noted among F1–F4 stages: platelet count, γ-globulin, α-2-macroglobulin, haptoglobin, hyaluronic acid, TIMP-2 and type IV collagen 7S.

Significant variables serving staging of hepatitis

Univariate analyses using trend analysis with the Cochran–Armitage method showed that the fibrotic stage of chronic hepatitis B (FSB) was significantly correlated with platelet count (Spearman: $r = -0.45$, $P < 0.001$), γ-GTP ($r = 0.19$, $P = 0.017$), γ-globulin ($r = 0.29$, $P < 0.001$), α-2-macroglobulin ($r = 0.32$, $P < 0.001$), hyaluronic acid ($r = 0.36$, $P < 0.001$), TIMP-2 ($r = 0.16$, $P = 0.043$), procollagen III peptide ($r = 0.30$, $P < 0.001$) and type IV collagen 7S ($r = 0.55$, $P < 0.001$).

Regression function generated from training patient group

After stepwise variable selection, multivariate regression analysis finally obtained the following function: $z = 1.40 \times ln$ (type IV collagen 7S) (ng/mL) $- 0.017 \times$ (platelet count) ($\times 1000^3/mm^3$) $+ 1.24 \times ln$ (TIMP-2) (ng/mL) $+ 1.19 \times ln$ (α-2-macroglobulin) (mg/dL) $- 9.15$. Median values of the fibrosis score of F1 ($n = 73$), F2 ($n = 42$), F3 ($n = 31$) and F4 stages ($n = 12$) were calculated as 0.95, 2.07, 2.98 and 3.63, respectively

Table 1 Demography and laboratory data of 158 patients in training group

	F1 ($n = 73$)	F2 ($n = 42$)	F3 ($n = 31$)	F4 ($n = 12$)
Demographics				
Men : women	58:15	33:9	23:8	10:2
Age (median, range)	36 (16–70)	39.5 (18–66)	39 (25–64)	43 (32–59)
Laboratory data (median, range)				
WBC (×1000/mm³)	5.4 (2.5–10.6)	5.1 (2.4–8.7)	4.9 (3.0–8.7)	4.1 (3.7–6.6)
Hemoglobin (g/dL)	15.3 (10.3–18.8)	15.4 (12.5–17.9)	15.2 (11.5–17.2)	14.45 (12.1–18.2)
Platelet (×1000/mm³)	204 (124–341)	173 (82–308)	155 (96–220)	130 (86–230)
Albumin (g/dL)	4.1 (3.2–4.9)	4.0 (3.2–5.1)	4.0 (3.3–4.9)	3.95 (3.4–4.6)
Bilirubin (mg/dL)	0.8 (0.2–1.7)	0.8 (0.3–2.3)	0.9 (0.4–5.4)	0.85 (0.6–2.3)
AST (IU/L)	48 (16–450)	55 (17–588)	54 (17–1446)	76.5 (27–396)
ALT (IU/L)	102 (10–839)	90 (12–886)	85 (19–2148)	89 (18–809)
γ-GTP (IU/L)	37 (7–247)	55 (8–687)	44 (14–564)	69 (33–262)
γ-Globulin (g/dL)	1.29 (0.78–2.11)	1.495 (0.62–3.20)	1.43 (0.90–2.30)	1.735 (0.92–2.47)
γ-Globulin (%)	17.3 (10.8–26.1)	19.3 (8.5–35.6)	19.9 (12.9–28.6)	22.55 (13.9–30.2)
α-2-Macroglobulin (mg/dL)	226 (116–446)	276 (148–495)	261 (202–565)	286.5 (166–425)
Haptoglobin (mg/dL)	77 (<5–318)	59 (<5–238)	61 (<5–151)	48.5 (<5–145)
Apolipoprotein A-I (mg/dL)	134 (89–212)	143 (78–250)	133 (87–189)	125 (73–169)
Hyaluronic acid (μg/L)	16 (<5–130)	32.5 (<5–204)	38 (<5–418)	49 (24–335)
TIMP-1 (ng/mL)	168 (93–271)	172 (116–314)	157 (119–365)	192 (145–365)
TIMP-2 (ng/mL)	80 (41–135)	80.5 (35–121)	92 (38–251)	85.5 (70–123)
Procollagen III peptide (U/mL)	0.75 (0.53–1.90)	0.835 (0.45–1.20)	0.89 (0.58–2.50)	1.05 (0.71–2.20)
Type IV collagen 7S (ng/ml)	4.0 (2.7–7.7)	4.6 (2.6–9.6)	5.6 (2.3–15.0)	7.2 (4.2–14.0)

ALT, alanine aminotransferase; AST, aspartate aminotransferase; γ-GTP, γ-glutamyl transpeptidase; TIMP, tissue inhibitor of matrix metalloproteinase; WBC, white blood cells.

(Fig. 1). The multiple regression coefficient and coefficient of determination were 0.646 ($P < 0.001$) and 0.418 ($P < 0.001$), respectively.

Because the generated regression function was obtained by multivariate analysis with stepwise variable selection, several variables were removed from the function due to multicollinearity among them. Mutual correlation among the fibrosis predictors are shown in Table 2.

A 28-year-old man of F1 fibrotic stage (Fig. 2a) had a serum type IV collagen concentration of 4.4 ng/mL, platelet 221×10^3 count/mm³, TIMP-2 75 ng/mL and α-2-macroglobulin 226 mg/dL. The regression function provided a fibrosis score of 0.99. Another man aged 46 years had F3 fibrosis on histological examination (Fig. 2b). His type IV collagen was 5.3 ng/mL, platelet 137×10^3 count/mm³, TIMP-2 92 ng/mL and α-2-macroglobulin 255, and the regression function calculated his fibrosis score as 3.10.

Validation of discriminant function

Validation data of 69 patients (Table 3) were collected from the other six institutions in Japan. When applying
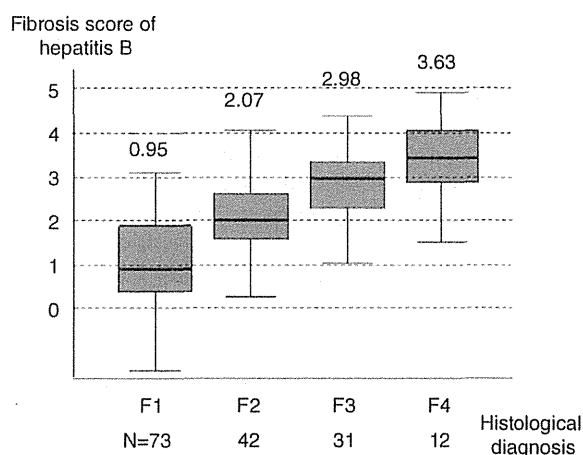
Figure 1 Box and whisker plots of fibrotic score of each histological fibrosis group in the training dataset. The fibrosis score of hepatitis B was generated by the function, z = 1.40 × *ln* (type IV collagen 7S) (ng/mL) – 0.017 × (platelet count) (×1000³/mm³) + 1.24 × *ln* (tissue inhibitor of matrix metalloproteinase-2) (ng/mL) + 1.19 × *ln* (α-2-macroglobulin) (mg/dL) – 9.15.

Table 2 Correlation coefficients (Spearman's ρ) among fibrosis predictors used in multivariate analysis

	Platelet	gamma-globulin	ln (α-2-macroglobulin)	ln (hyaluronate)	ln (P-III-P)	ln (IV collagen)	ln (TIMP-2)
Platelet (×10³/mm³)	1.000	-0.214 ($P = 0.008$)	-0.260 ($P = 0.001$)	-0.384 ($P < 0.001$)	-0.045 ($P = 0.58$)	-0.297 ($P < 0.001$)	0.094 ($P = 0.24$)
γ-Globulin (g/dL)		1.000	0.276 ($P = 0.001$)	0.349 ($P < 0.001$)	0.342 ($P < 0.001$)	0.414 ($P < 0.001$)	0.268 ($P = 0.001$)
ln (α-2-macroglobulin) (mg/dL)			1.000	0.281 ($P < 0.001$)	0.141 ($P = 0.078$)	0.171 ($P = 0.032$)	-0.079 ($P = 0.32$)
ln (hyaluronic acid) (mg/L)				1.000	0.373 ($P < 0.001$)	0.493 ($P < 0.001$)	0.089 ($P = 0.27$)
ln (procollagen III peptide) (U/mL)					1.000	0.600 ($P < 0.001$)	0.145 ($P = 0.071$)
ln (type IV collagen) (mg/L)						1.000	0.358 ($P < 0.001$)
ln (TIMP-2) (mg/L)							1.000

TIMP, tissue inhibitor of matrix metalloproteinase.

the regression function for the validation set, the fibrosis score demonstrated good reproducibility, showing 1.33 in patients with chronic hepatitis of F1 ($n = 27$), 2.20 of F2 ($n = 20$), 3.11 of F3 ($n = 20$) and 5.30 of F4 ($n = 2$), respectively (Fig. 3). Although F4 fibrosis stage consisted of only two patients and the score 5.30 was regarded as of rather higher value, the scores of other stages of fibrosis were concordant with histological fibrosis.

Comparisons of efficacy with various fibrosis scores (Fig. 4)

In order to evaluate the efficacy and usefulness of the obtained FSB, we compared it with previously reported fibrosis scores using training data. AAR, APRI and FibroTest showed only slight correlation with actual histological stage. FIB-4 demonstrated an increasing trend of the score associated with histological fibrosis, but significant overlapping scores were found in F1–F4. Spearman's correlation coefficients of AAR, APRI, FIB-4 and FibroTest were 0.199 ($P = 0.012$), 0.265 ($P = 0.001$), 0.412 ($P < 0.001$) and 0.330 ($P < 0.001$), respectively. Our FSB showed a Spearman's correlation coefficient of 0.625 ($P < 0.001$), and was a much higher value than the others. The dichotomous discrimination function for cirrhosis and hepatitis C in Japanese patients[23] showed good differentiation also in patients with hepatitis B virus.

DISCUSSION

RECOGNITION OF SEVERITY of chronic hepatitis is essential in managing patients with chronic HBV infection: estimation of length of infection, existence of any previous hepatitis activity, presumption of current fibrotic stage, and prediction of future fibrosis progression and hepatocarcinogenesis. Differential diagnosis of cirrhosis from chronic hepatitis is especially important in the evaluation of chronic HBV infection. Identification of liver cirrhosis often leads to an important change in management of the patient: need for fiberscopic examination for esophageal varices, ultrasonographic exploration for the association of liver cancer, and prediction of hepatic decompensation. Guidelines published by the American Association of Study of Liver Disease[24] recommend liver biopsy for HBV carriers with aminotransferase elevation or for any candidates of antiviral therapy, because hepatic fibrosis sometimes shows unexpectedly far advancement to cirrhosis, and because it is very difficult to evaluate and translate the liver function tests or ultrasonographic findings compared to chronic hepatitis type C.

Table 3 Demography and laboratory data of 69 patients in training group

	F1 ($n = 27$)	F2 ($n = 20$)	F3 ($n = 20$)	F4 ($n = 2$)
Demographics				
Men : women	18:9	15:5	13:7	2:0
Age (median, range)	36 (13–64)	45 (14–64)	36.5 (24–59)	32 (25–39)
Laboratory data (median, range)				
WBC (×1000/mm³)	5.0 (2.8–8.7)	5.8 (2.8–11.6)	5.3 (3.2–8.1)	3.85 (2.7–5.0)
Hemoglobin (g/dL)	14.8 (12.4–17.4)	15.0 (12.4–16.9)	14.4 (11.1–16.4)	14.4 (12.5–16.3)
Platelet (×1000/mm³)	204 (86–322)	180 (90–275)	147 (90–276)	130 (67–183)
Albumin (g/dL)	4.4 (2.8–5.2)	4.2 (3.5–5.1)	4.3 (3.4–4.9)	4.45 (4.0–4.9)
Bilirubin (mg/dL)	0.9 (0.4–6.4)	0.8 (0.2–1.6)	0.75 (0.4–1.7)	1.15 (1.1–1.2)
AST (IU/L)	52 (17–575)	50.5 (21–272)	65 (22–284)	248.5 (51–446)
ALT (IU/L)	84 (16–1101)	101.5 (19–554)	86.5 (16–1113)	453.5 (74–833)
γ-GTP (IU/L)	42 (14–332)	54 (16–205)	52.5 (13–191)	193 (57–329)
γ-Globulin (g/dL)	1.30 (1.04–1.59)	1.35 (1.18–2.53)	1.62 (1.16–1.97)	1.545 (1.51–1.58)
γ-Globulin (%)	17.9 (14.3–22.1)	19.6 (15.5–30.8)	22.0 (16.5–24.6)	20.15 (19.3–21.0)
α-2-Macroglobulin (mg/dL)	287 (160–687)	270 (89–452)	272.5 (211–463)	389 (313–465)
Haptoglobin (mg/dL)	58 (<5–229)	74 (<5–154)	56.5 (<5–198)	<5 (<5–<5)
Apolipoprotein A-I (mg/dL)	146 (95–216)	137 (87–162)	120 (88–170)	100.5 (74–127)
Hyaluronic acid (µg/L)	27 (<5–113)	36 (10–1050)	59 (14–439)	331 (225–437)
TIMP-1 (ng/mL)	168.5 (83–302)	176 (127–408)	182 (104–303)	390.5 (283–498)
TIMP-2 (ng/mL)	76 (25–143)	86.5 (28–154)	77.5 (32–141)	100.5 (91–110)
Procollagen III peptide (U/mL)	0.71 (0.27–2.20)	0.88 (0.63–2.80)	0.995 (0.60–2.10)	1.75 (1.50–2.00)
Type IV collagen 7S (ng/ml)	3.6 (2.7–17.0)	5.25 (3.3–13.0)	5.7 (3.0–16.0)	15.5 (15.0–16.0)

ALT, alanine aminotransferase; AST, aspartate aminotransferase; γ-GTP, γ-glutamyl transpeptidase; TIMP, tissue inhibitor of matrix metalloproteinase; WBC, white blood cells.

Recently, non-invasive estimation of severity of liver fibrosis has been reported in patients with HBV-related chronic hepatitis.[2,6–13] However, these studies were principally aimed at differentiation of advanced fibrotic stages of F3 or F4 from mild fibrotic stages of F1 or F2. Those discrimination functions were insufficient to recognize the stepwise progression of viral hepatitis from F1–F4. This dichotomy (mild or severe) of chronic hepatitis B seemed less valuable in the study of disease progression, disease control abilities of antiviral drugs and estimation of histological improvement after anti-inflammatory drugs. A histology-oriented, practical and reliable formula is therefore required for the diagnosis and investigation of chronic hepatitis B.

This study aimed to establish non-invasive evaluation and calculation of liver fibrosis for patients with chronic hepatitis B virus infection. Although it was retrospectively performed as a multicenter study of eight institutions, judgment of histological diagnosis was independently performed by four pathologists in another hospital, who were informed only of the patient's age, sex and positive HBV infection. Objective judgment of the histological staging and grading in sufficient biopsy specimens could be obtained.
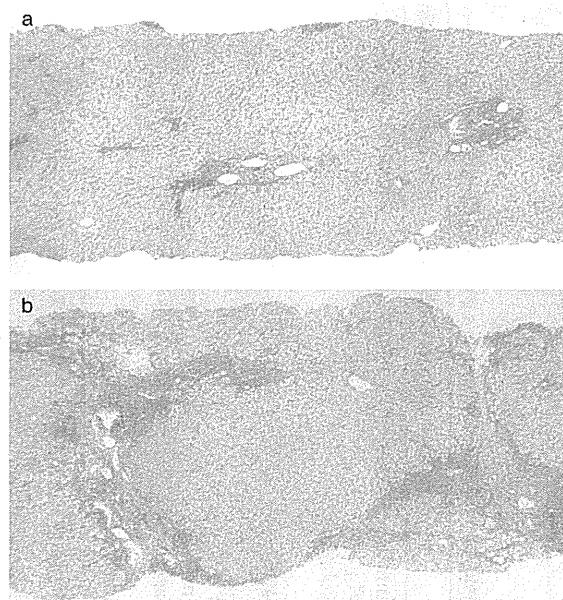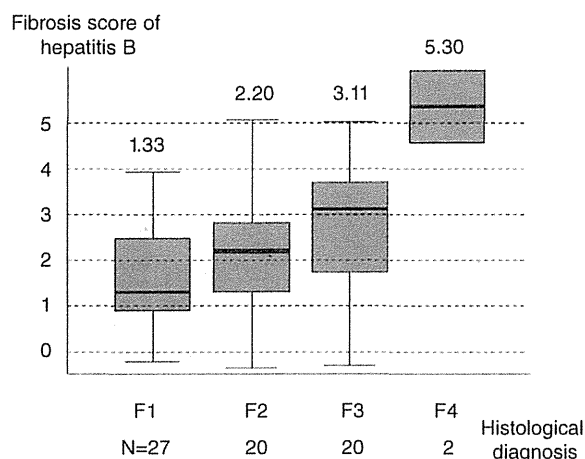

Figure 2 Case presentations of the training set. (a) A 28-year-old man with F1 fibrosis. Final regression function provided his fibrosis score as 0.99. (b) A 45-year-old man with F3 fibrosis. His regression coefficient was calculated as 3.10. Silver stain, ×40.

© 2012 The Japan Society of Hepatology

Figure 3 Box and whisker plots of fibrotic score of each group of histological fibrosis in the validation dataset. The fibrosis score of hepatitis B was generated by the function, $z = 1.40 \times ln$ (type IV collagen 7S) (ng/mL) $- 0.017 \times$ (platelet count) ($\times 1000^3/mm^3$) $+ 1.24 \times ln$ (tissue inhibitor of matrix metalloproteinase-2) (ng/mL) $+ 1.19 \times ln$ (α-2-macroglobulin) (mg/dL) $- 9.15$.

As many as 227 patients with chronic hepatitis B were analyzed in this study, who had been diagnosed as having chronic hepatitis or cirrhosis by liver biopsy performed in experienced liver units in Japan. To obtain the most suitable equation approximating histological fibrotic stage, multivariate analysis was performed using two demographic parameters (age and sex) and 21 hematological and biochemical markers with or without logarithmic transformation. They included many kinds of fibrosis markers: α-2-macroglobulin, haptoglobin concentration, haptoglobin typing, apolipoprotein A1, hyaluronic acid, TIMP-1, TIMP-2, procollagen III peptide and type IV collagen 7S Multiple regression analysis finally generated a first-degree polynomial function consisting of four variables: type IV collagen 7S, platelet count, TIMP-2 and α2-macroglobulin. A constant numeral (-9.15) was finally adjusted in the regression equation in order to obtain fitted figures for a fibrotic stage of F1–F4. From the magnitude of the standardized partial regression coefficient of individual variable in the function, platelet count demonstrated the most potent contribution toward the prediction of liver fibrosis. Type IV collagen 7S and ln (TIMP-2) proved to be the second and third distinctive power in the model, respectively.

The FSB was sufficiently fitted to actual fibrotic stages with certain overlapping as is usually found in histological ambiguity judged by pathologists. Because judgment of fibrosis in chronic hepatitis often shows a transitional

histological staging, pathological examination cannot always make a clear-cut diagnosis discriminating F1–F4. Considering the limitation of the pathological difficulty in differentiating the four continuous disease entities, the obtained regression function showed satisfactory high accuracy rates in the prediction of liver disease severity. The FSB can provide one or two decimal places (e.g. 3.2 or 3.24) and the utility of the score is possibly higher than the mere histological stage of F1–F4. The reproducibility was confirmed by the remaining 67 patients' data obtained from the other six hospitals. Although the validation data were collected from a different geographic area and different chronological situation, the FSB showed similar results in prediction of histological staging.

The FSB seemed a very useful quantitative marker in evaluating fibrotic severity of hepatitis B patients without invasive procedures and without any specialized ultrasonography or magnetic resonance imaging. The FSB also has an advantage of measurement, in which old blood samples are available for retrospective assessment of varied clinical settings: for example, old sera from 20 years prior to the time of initial liver biopsy, or paired sera before and after long-term antiviral therapy. These kinds of retrospective assessments of fibrotic staging will be valuable in estimating a long-term progression of liver disease, in evaluating efficacy of long-term medication or other medical intervention, or in making a political judgment from the viewpoints of socioeconomic efficacy.

The score can be calculated for any patients with chronic HBV infection. Although this multiple regression model dealt with appropriate logarithmic transformation for non-normal distribution parameters, the regression analysis was based on a linear regression model. Very slight fibrosis can be calculated as less than 1.00, which is commonly found to a slight degree in chronic hepatitis with tiny fibrotic change as F0. Very severe fibrosis might be calculated as more than 4.00, which is an imaginary and nonsense number in the scoring system of fibrosis. The FSB is, however, very useful and valuable in a real clinical setting: estimation of severity of liver fibrosis in an outpatient clinic, evaluation of the natural progression of a patient's fibrosis over 10 years and assessment of a long-term administration of interferon in patients with chronic hepatitis B from the viewpoint of fibrotic change. Recent development of new nucleoside/nucleotide analogs requires evaluation for long-term histological advantage, for aggravation of hepatitis stage during viral and biochemical breakthrough caused by HBV mutation, and even for
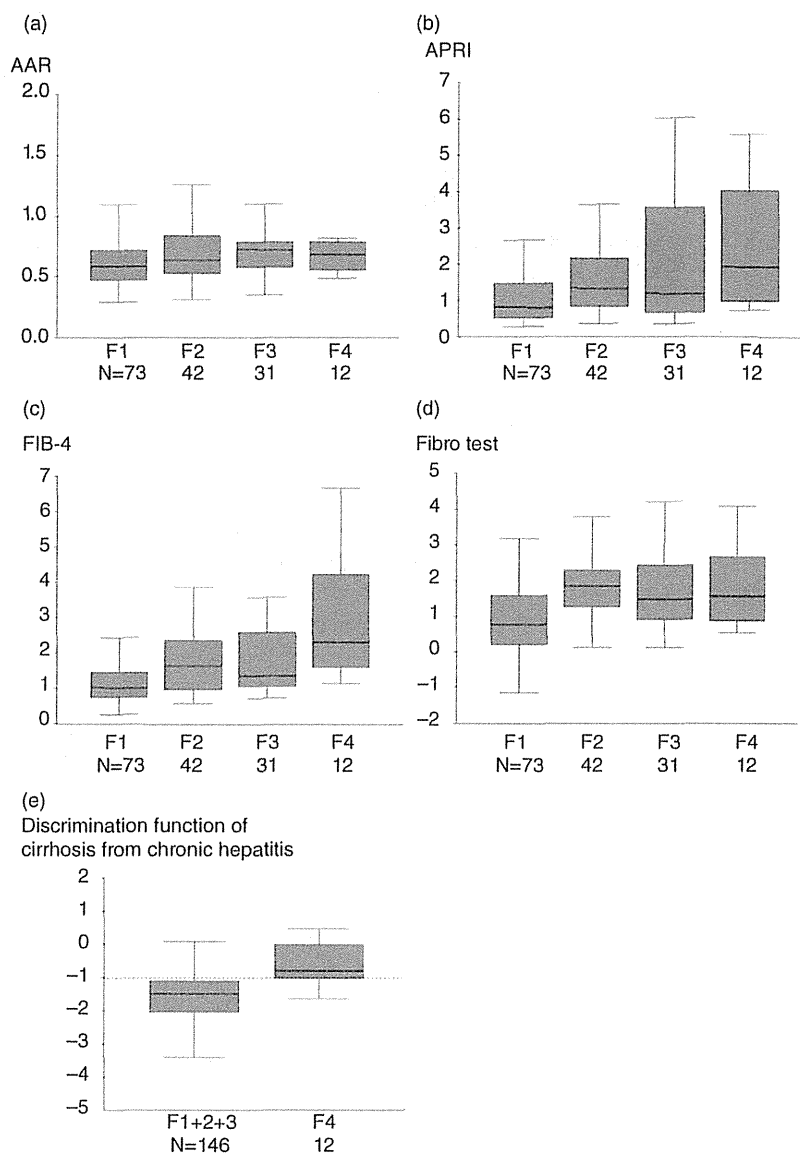
Figure 4 Previously published fibrosis scores. (a) Aspartate aminotransferase/ alanine aminotransferase ratio (AAR),[19] (b) aspartate aminotransferase-to-platelet ratio index (APRI),[20] (c) FIB-4,[21] (d) FibroTest[22] and (e) discrimination function of cirrhosis from hepatitis in Japanese patients.[23]

the best management of patients with chronic hepatitis B. The FSB seems one of the ideal methods of approximating the fibrotic stage of chronic hepatitis B. Repeated measurement is quite suitable for patients with an unestablished treatment or trial, every 1 or 2 years, for example. Because the current regression function was generated from the data of HBV-related chronic liver disease, this equation would not be suitable for the recognition of hepatitis C virus-related chronic liver disease, alcoholic liver disease, and other congenital or autoimmune liver diseases. To recognize the latter diseases, other studies of individual diseases must be performed.

We compared the usefulness of the FSB with that of other fibrosis scores.[19–23] The more simple and less expensive AAR or APRI could not estimate fibrotic stages with poor correlation coefficients of 0.199 and 0.265, which are much lower than the coefficient of the FSB of 0.625. FibroTest, which contained three costly fibrosis markers (α-2-macroglobulin, haptoglobin and apolipo-

protein A1), also showed a low correlation coefficient of 0.330, suggesting that its usefulness was limited in HBV positive oriental patients. Although FIB-4 demonstrated the best coefficient of 0.412 among the fibrosis scores, significant overlaps were found between neighboring stages and obtained scores were not coordinated for real histological classification.

In conclusion, the FSB was a useful and reliable biomarker for prediction of liver fibrosis in patients with chronic HBV infection. The FSB is expected to be introduced and utilized in varied kinds of studies and trials. Its accuracy and reproducibility require further validation using higher numbers of patients in several countries other than Japan.

ACKNOWLEDGMENTS

REFERENCES

1 Sandrin L, Fourquet B, Hasquenoph JM *et al.* Transient elastography: a new noninvasive method for assessment of hepatic fibrosis. *Ultrasound Med Biol* 2003; 29: 1705–13.

2 Myers RP, Tainturier MH, Ratziu V *et al.* Prediction of liver histological lesions with biochemical markers in patients with chronic hepatitis B. *J Hepatol* 2003; 39: 222–30.

3 Hanna RF, Kased N, Kwan SW *et al.* Double-contrast MRI for accurate staging of hepatocellular carcinoma in patients with cirrhosis. *AJR Am J Roentgenol* 2008; 190: 47–57.

4 Hagiwara M, Rusinek H, Lee VS *et al.* Advanced liver fibrosis: diagnosis with 3D whole-liver perfusion MR imaging-initial experience. *Radiology* 2008; 246: 926–34.

5 Taouli B, Chouli M, Martin AJ, Qayyum A, Coakley FV, Vilgrain V. Chronic hepatitis: role of diffusion-weighted imaging and diffusion tensor imaging for the diagnosis of liver fibrosis and inflammation. *J Magn Reson Imaging* 2008; 28: 89–95.

6 Montazeri G, Estakhri A, Mohamadnejad M *et al.* Serum hyaluronate as a non-invasive marker of hepatic fibrosis and inflammation in HBeAg-negative chronic hepatitis B. *BMC Gastroenterol* 2005; 5: 32.

7 Zeng MD, Lu LG, Mao YM *et al.* Prediction of significant fibrosis in HBeAg-positive patients with chronic hepatitis B by a noninvasive model. *Hepatology* 2005; 42: 1437–45.

8 Chrysanthos NV, Papatheodoridis GV, Savvas S *et al.* Aspartate aminotransferase to platelet ratio index for fibrosis evaluation in chronic viral hepatitis. *Eur J Gastroenterol Hepatol* 2006; 18: 389–96.

9 Kim BK, Kim Y, Park JY *et al.* Validation of FIB-4 and comparison with other simple noninvasive indices for predicting liver fibrosis and cirrhosis in hepatitis B virus-infected patients. *Liver Int* 2010; 30: 546–53.

10 Wu SD, Wang JY, Li L. Staging of liver fibrosis in chronic hepatitis B patients with a composite predictive model: a comparative study. *World J Gastroenterol* 2010; 16: 501–7.

11 Sökücü S, Gökçe S, Güllüoğlu M, Aydoğan A, Celtik C, Durmaz O. The role of the non-invasive serum marker FibroTest-ActiTest in the prediction of histological stage of fibrosis and activity in children with naïve chronic hepatitis B infection. *Scand J Infect Dis* 2010; 42: 699–703.

12 Liu HB, Zhou JP, Zhang Y, Lv XH, Wang W. Prediction on liver fibrosis using different APRI thresholds when patient age is a categorical marker in patients with chronic hepatitis B. *Clin Chim Acta* 2011; 412: 33–7.

13 Park SH, Kim CH, Kim DJ *et al.* Usefulness of Multiple Biomarkers for the Prediction of Significant Fibrosis in Chronic Hepatitis B. *J Clin Gastroenterol* 2011; 45: 361–5.

14 Engstrom-Laurent A, Loof L, Nyberg A, Schroder T. Increased serum levels of hyaluronate in liver disease. *Hepatology* 1985; 5: 638–42.

15 Murawaki Y, Ikuta Y, Koda M, Kawasaki H. Serum type III procollagen peptide, type IV collagen 7S domain, central triple-helix of type IV collagen and tissue inhibitor of metalloproteinases in patients with chronic viral liver disease: relationship to liver histology. *Hepatology* 1994; 20: 780–7.

16 Fabris C, Falleti E, Federico E, Toniutto P, Pirisi M. A comparison of four serum markers of fibrosis in the diagnosis of cirrhosis. *Ann Clin Biochem* 1997; 34: 151–5.

17 Desmet VJ, Gerber M, Hoofnagle JH, Manns M, Sheuer PJ. Classification of chronic hepatitis: diagnosis, grading, and staging. *Hepatology* 1994; 19: 1513–20.

18 IBM SPSS Inc. *IBM SPSS for Windows Version 19.0 Manual.* Armonk NY, USA: SPSS Japan Inc., an IBM company, 2009.

19 Sheth SG, Flamm SL, Gordon FD *et al.* AST/ALT ratio predicts cirrhosis in patients with chronic hepatitis C virus infection. *Am J Gastroenterol* 1998; 93: 44–8.

20 Wai CT, Greenson JK, Fontana RJ *et al.* A simple noninvasive index can predict both significant fibrosis and cirrhosis in patients with chronic hepatitis C. *Hepatology* 2003; 38: 518–26.

21 Sterling RK, Lissen E, Clumeck N *et al.* Develoment of a simple noninvasive index to predict significant fibrosis in patients with HIV/HCV coinfection. *Hepatology* 2006; 43: 1317–25.

22 Imbert-Bismut F, Ratziu V, Pieroni L *et al.* Biochemical imarkers of liver fibrosis in patients with hepatitis C virus infection: a prospective study. *Lancet* 2001; 357: 1069–75.

23 Ikeda K, Saitoh S, Kobayashi M *et al.* Distinction between chronic hepatitis and liver cirrhosis in patients with hepatitis C virus infection. Practical Discriminant function using common laboratory data. *Hepatol Res* 2000; 18: 252–66.

24 Lok ASF, McMahon BJ. AASLD Practice Guidelines. Chronic hepatitis B: update 2009. *Hepatology* 2009; 50: 1–36.

A genome-wide association study of HCV-induced liver cirrhosis in the Japanese population identifies novel susceptibility loci at the MHC region

Yuji Urabe[1,2], Hidenori Ochi[2], Naoya Kato[4], Vinod Kumar[1,3], Atsushi Takahashi[3],
Ryosuke Muroyama[4], Naoya Hosono[3], Motoyuki Otsuka[5], Ryosuke Tateishi[5], Paulisally Hau Yi Lo[1],
Chizu Tanikawa[1], Masao Omata[5], Kazuhiko Koike[5], Daiki Miki[2], Hiromi Abe[2], Naoyuki Kamatani[3],
Joji Toyota[6], Hiromitsu Kumada[7], Michiaki Kubo[3], Kazuaki Chayama[2], Yusuke Nakamura[1,3],
Koichi Matsuda[1,*]

[1]Laboratory of Molecular Medicine, Human Genome Center, Institute of Medical Science, The University of Tokyo, Tokyo, Japan; [2]Department of Medical and Molecular Science, Division of Frontier Medical Science, Programs for Biomedical Research, Graduate School of Biomedical Sciences, Hiroshima University, Hiroshima, Japan; [3]Center for Genomic Medicine, The Institute of Physical and Chemical Research (RIKEN), Kanagawa, Japan; [4]Unit of Disease Control Genome Medicine, The Institute of Medical Science, The University of Tokyo, Tokyo, Japan; [5]Department of Gastroenterology, Graduate School of Medicine, The University of Tokyo, Tokyo, Japan; [6]Department of Gastroenterology, Sapporo Kosei General Hospital, Hokkaido, Japan; [7]Department of Hepatology, Toranomon Hospital, Tokyo, Japan

Background & Aims: We performed a genome-wide association study (GWAS) of hepatitis C virus (HCV)-induced liver cirrhosis (LC) to identify predictive biomarkers for the risk of LC in patients with chronic hepatitis C (CHC).
Methods: A total of 682 HCV-induced LC cases and 1045 CHC patients of Japanese origin were genotyped by Illumina Human Hap 610-Quad bead Chip.
Results: Eight SNPs which showed possible associations ($p < 1.0 \times 10^{-5}$) at the GWAS stage were further genotyped using 936 LC cases and 3809 CHC patients. We found that two SNPs within the major histocompatibility complex (MHC) region on chromosome 6p21, rs910049 and rs3135363, were significantly associated with the progression from CHC to LC ($p_{combined} = 9.15 \times 10^{-11}$ and 1.45×10^{-10}, odds ratio (OR) = 1.46 and 1.37, respectively). We also found that HLA-DQA1*0601 and HLA-DRB1*0405 were associated with the progression from CHC to LC ($p = 4.53 \times 10^{-4}$ and 1.54×10^{-4} with OR = 2.80 and 1.45, respectively). Multiple logistic regression analysis revealed that rs3135363, rs910049, and HLA-DQA1*0601 were independently associated with the risk of HCV-induced LC. In addition, individuals with four or more risk alleles for these three loci have a 2.83-fold higher risk for LC than those with no risk allele, indicating the cumulative effects of these variations.
Conclusions: Our findings elucidated the crucial roles of multiple genetic variations within the MHC region as prognostic/predictive biomarkers for CHC patients.
© 2013 European Association for the Study of the Liver. Published by Elsevier B.V. All rights reserved.

Introduction

Two million people in Japan and 210 million people worldwide are estimated to be infected with the hepatitis C virus (HCV), which is known to be a major cause of chronic viral liver disease [1]. Patients with chronic hepatitis C (CHC) usually exhibit mild inflammatory symptoms, but are at a significantly high risk for developing liver cirrhosis (LC) and hepatocellular carcinoma [2]. More than 400,000 people at present suffer from LC, which is ranked as the 9th major cause of death in Japan. In addition, liver cancer causes approximately 32,000 deaths per year, making it the 4th most common cause of death from malignant diseases. Thus, HCV-related diseases are important public health problems [3].

Clinical outcomes after the exposure to HCV vary enormously among individuals. Approximately 70% of infected persons will develop chronic hepatitis [4], and about 20–30% of CHC patients will develop cirrhosis, but others can remain asymptomatic for decades [2]. The annual death rate of patients with decompensated cirrhosis is as high as 15–30% [5]. Moreover, more than 7% of LC patients develop hepatocellular cancer in Japan and Taiwan, while the frequencies are less than 1.6% among other ethnic groups [6,7]. These inter-individual and inter-ethnic differences have been attributed to various factors such as viral genotypes,

ELSEVIER

Viral Hepatitis

Research Article

Table 1. Characteristics of samples and methods used in this study.

Stage	Source	Platform	Number of samples	Female (%)	Age, yr (mean ± SD)
GWAS					
Liver cirrhosis	BioBank Japan	Illumina Human Hap 610	682	313 (46.3)	67.1 ± 9.7
Chronic hepatitis C[a]	Hiroshima University	Illumina Human Hap 610	1045	371 (35.5)	55.2 ± 11.0
Replication					
Liver cirrhosis	Tokyo University	Invader assay	716	334 (46.8)	64.4 ± 10.4
	Hiroshima University		220	98 (44.5)	64.7 ± 8.98
Chronic hepatitis C[a]	BioBank Japan	Invader assay	1670	780 (46.8)	59.7 ± 12.6
	Hiroshima University		2139	1061 (51.8)	58.8 ± 9.20

[a]Number of samples that qualified. CHC patients with severe liver fibrosis (F3 or F4) or lower platelet counts (<160,000) were excluded.

alcohol consumption, age at infection, co-infection of HIV or HBV [8–10], insulin resistance, steatosis, and metabolic syndrome [11]. Previous gene expression analyses also identified various genes associated with liver fibrosis among patients with CHC [12–14]. In addition, miRNAs such as mir-21 and mir-122 were shown to be correlated with live fibrosis [15,16].

Currently, the genome-wide association study is the most common method to identify genetic variations associated with disease risk [17–20]. In addition, the roles of genetic factors in HCV-related diseases have been elucidated. *IL28B* is associated with spontaneous clearance of HCV [21] as well as with the clinical response to the combination therapy of pegylated interferon and ribavirin [22,23]. Recently, our group has shown that SNP rs2596542 on *MICA* [24] and SNP rs1012068 on *DEPDC5* [25] are significantly associated with HCV-induced liver cancer. Although liver cirrhosis is the major risk factor of liver cancer, a fraction of CHC patients will develop HCC without accompanying LC. Therefore, the underlying genetic background would be different between HCV-induced LC and HCV-induced HCC. Previous studies identified the association of genetic variants in *HLA-DQ/DR/B* [26–28], *2–5AS* [29], *TLR3* [30], and *PNPLA3* [31] with the risk of liver fibrosis among patients with CHC. However, a comprehensive approach for HCV-induced LC has not been conducted so far. Here we performed GWAS of HCV-induced LC to identify predictive biomarkers for the risk of LC in patients with CHC.

Materials and methods

Ethics statement

All subjects provided written informed consent. This project was approved by the ethical committees at University of Tokyo, Hiroshima University, Sapporo Kosei General Hospital, Toranomon Hospital, and Center for Genomic Medicine, Institutes of Physical and Chemical Research (RIKEN).

Study population

The characteristics of each cohort are shown in Table 1. In this study, we conducted GWAS and replication analysis on a total of 1618 HCV-induced LC and 4854 CHC patients. All subjects had abnormal levels of serum alanine transaminase for more than 6 months and were positive for both HCV antibody and serum HCV RNA. Among 1618 LC and 4854 CHC samples, 342 LC patients (21.14%) and 2997 CHC patients (61.70%) underwent liver biopsy. The remaining 1276 LC and 1857 CHC patients were diagnosed by non-invasive methods including hepatic imaging (e.g., ultrasonography, computed tomography, arteriography or magnetic resonance imaging), biochemical data (serum bilirubin, serum albumin, platelet, or prothrombin time), and the presence/absence of clinical manifestations of portal hypertension (e.g., varices, encephalopathy or ascites). The patients with CHC

or LC were recruited for this study regardless of their treatment history. We excluded from the analysis the followings CHC patients: (1) advanced liver fibrosis (F3 or F4 by New Inuyama classification) [32], (2) platelet count under 160,000 for patients without liver fibrosis staging, and (3) HBV co-infection. Characteristics of each study cohort are shown in Table 1. In brief, DNA of HCV-induced LC and CHC patients was obtained from Biobank Japan (http://biobankjp.org/) [33], the Hiroshima Liver Study Group (http://home.hiroshima-u.ac.jp/naika1/researchprofile/pdf/liverstudygroupe.pdf), Toranomon Hospital, and the University of Tokyo. All subjects were of Japanese origin.

SNP genotyping

Genomic DNA was extracted from peripheral blood leukocytes using a standard method. In GWAS, we genotyped 682 LC and 1045 CHC samples using Illumina Human Hap 610-Quad bead Chip (Supplementary Fig. 1). Samples with low call rate (<0.98) were excluded from our analysis (six LC and two CHC samples). We then applied SNP quality control as follows: call rate ≥0.99 in LC and CHC samples, Hardy–Weinberg $p \geqslant 1 \times 10^{-6}$ in LC and CHC samples. Consequently, 461,992 SNPs on the autosomal chromosomes passed the quality control filters. SNPs with minor allele frequency of <0.01 in both LC and CHC samples were excluded from further analyses, considering statistical power in the replication analysis. Finally, we analyzed 431,618 SNPs in GWAS. Among the top ten SNPs showing $p < 1.0 \times 10^{-5}$, we selected nine SNPs for further analysis with LD threshold of $r^2 = 0.95$. In the replication stage, we genotyped 936 LC and 3809 CHC using multiplex PCR-based Invader assay (Third Wave Technologies).

Statistical analysis

The association of SNPs with the phenotype in the GWAS, replication stage, and combined analyses was tested by logistic regression analysis, upon adjusting for age at recruitment (continuous) and gender, by assuming additive model using PLINK [34]. In the GWAS, the genetic inflation factor λ was derived by applying logistic regressed p values for all the tested SNPs. The quantile–quantile plot was drawn using R program. The odds ratios were calculated using the non-susceptible allele as reference, unless stated otherwise. The combined analysis of GWAS and replication stage was verified by using the Mantel–Haenszel method. We set the significance threshold as follows; $p = 1 \times 10^{-5}$ in the GWAS stage (first stage) and $p = 6.25 \times 10^{-3}$ (=0.05/8) in the replication analysis. We considered $p < 5 \times 10^{-8}$ as threshold of GWAS significance in the combined analysis, which is the Bonferroni-corrected threshold for the number of independent SNPs genotyped in HapMap Phase II [35]. The heterogeneity across two stages was examined by using the Breslow–Day test [36]. We used Haploview software to analyze the association of haplotypes and LD values between SNPs. Quality control for SNPs was applied as follows: call rate ≥0.95 in LC and CHC samples, and Hardy–Weinberg $p \geqslant 1 \times 10^{-6}$ in CHC samples in replication stage. The statistical power was 19.51% in GWAS (the first stage) ($p = 1.00 \times 10^{-5}$), 97.98% in replication ($p = 0.05/8$), and 74.76% in the combined stage ($p = 5.00 \times 10^{-8}$) at minor allele frequency of 0.3 and OR of 1.3.

Imputation-based association analysis of HLA class I and class II alleles

We obtained an SNP or a combination of SNPs which could tag the HLA alleles in the Japanese population from a previous study [37]. Genotypes of tagging SNPs were imputed in the GWAS samples by using a Hidden Markov model programmed in MACH [38] and haplotype information from HapMap JPT samples

876

Journal of Hepatology **2013** vol. 58 | 875–882

193
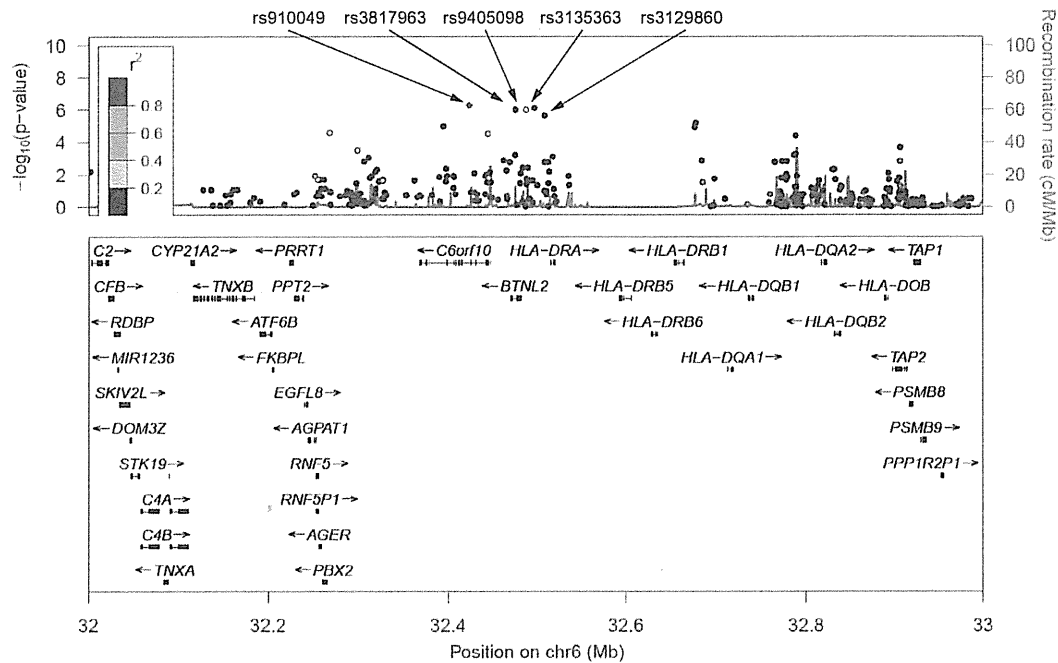
Fig. 1. **Regional association plot at 6p21.3.** (Upper panel) *p* Values of genotyped SNPs (circle) and imputed SNPs (cross) are plotted (as $-\log_{10} p$ value) against their physical position on chromosome 6 (NCBI Build 36). The *p* value for rs910049 at GWAS is represented by a purple diamond. Estimated recombination rates from HapMap JPT show the local LD structure. Inset; the color of the other SNPs indicates LD with rs3135363 according to a scale from $r^2 = 0$ to $r^2 = 1$ based on pair-wise r^2 values from HapMap JPT. (Lower panel) Gene annotations from the University of California Santa Cruz genome browser.

and 1000 genome imputation samples [39]. We applied the same SNP quality criteria as in GWAS, to select SNPs for the analysis. We employed the logistic regression analysis upon age and gender adjustment to assess the associations between HCV-induced LC and HLA alleles.

Software

For general statistical analysis, we employed R statistical environment version 2.9.1 (cran.r-project.org) or plink-1.06 (pngu.mgh.harvard.edu/~purcell/plink/). The Haploview software version 4.2 [40] was used to calculate LD and to draw Manhattan plot. Primer3 -web v0.3.0 (http://frodo.wi.mit.edu) web tool was used to design primers. We employed LocusZoom (http://csg.sph.umich.edu/locuszoom/) for regional plots. We used SNP Functional Prediction web tool for functional annotation of SNPs (http://snpinfo.niehs.nih.gov/snpfunc.htm) [41]. We used "Gene Expression Analysis Based on Imputed Genotypes" (http://www.sph.umich.edu/csg/liang/imputation) [42] for eQTL analysis. We used MACTH [43] web tool for searching potential binding sites for transcription factors (http://www.gene-regulation.com/index.htm).

Results

Genome-wide association study for HCV-induced liver cirrhosis

We performed a two-stage GWAS using a total of 1618 cases and 4854 controls (Supplementary Fig. 1). In the first stage, a whole genome scan was performed on 682 Japanese patients with HCV-induced LC and 1045 Japanese patients with CHC, using Illumina Human Hap 610-Quad bead Chip. The genotyping results of 431,618 single nucleotide polymorphisms (SNPs) obtained after our standard quality control were used for further analysis.

CHC patients with severe liver fibrosis (F3 or F4 according to the New Inuyama classification [32]) or lower platelet counts (<160,000) were excluded from the control group. As progression from CHC to LC is strongly affected by age and gender, we performed logistic regression analyses including age and gender as covariates at all tested loci in our analyses. The genetic inflation factor lambda was 1.051, indicating that there is little or no evidence of population stratification (Supplementary Fig. 2A). Although no SNPs cleared the GWAS significance threshold ($p < 5 \times 10^{-8}$) at the first stage, we selected ten candidate SNPs showing suggestive association of $p < 1 \times 10^{-5}$ (Supplementary Fig. 2B and Supplementary Table 1). After excluding SNP rs6891116 due to almost absolute linkage with SNP rs10252674 ($r^2 = 0.99$), the remaining nine SNPs were further genotyped using an independent cohort, consisting of 936 LC and 3809 CHC cases, by multiplex PCR-based Invader assay as the second stage. We could successfully obtain genotype results for eight SNPs after the QC filter (call rate $\geqslant 0.95$ in LC and CHC samples, Hardy–Weinberg of $p \geqslant 1 \times 10^{-6}$ in CHC samples). The logistic regression analysis adjusted by age and gender revealed that five SNPs on chromosome 6q21.3 indicated a significant association with progression from CHC to LC after the Bonferroni correction ($p < 0.05/8 = 6.25 \times 10^{-3}$, Supplementary Table 2). A meta-analysis of the two stages with a fixed-effects model revealed that all of the five SNPs significantly associated with progression from CHC to LC (p values of 9.15×10^{-11}– 1.28×10^{-8} with odds ratios (OR) of 1.30–1.46, Fig. 1 and Table 2). These five SNPs were located in the HLA class II region and were in strong linkage disequilibrium with each other ($D' > 0.75$,

Table 2. Summary of GWAS and replication analyses.

SNP	Stage	Allele (1/2)	Gene	Liver cirrhosis				Chronic hepatitis C				OR (95% CI)[b]	p value[c]	p value$_{het}$[d]
				11	12	22	RAF[a]	11	12	22	RAF[a]			
rs910049														
	GWAS	a/g	C6orf10 (6p21.3)	24	217	435	0.196	25	224	794	0.131	1.73 (1.40-2.15)	5.39 x 10⁻⁷	
	Replication			38	259	631	0.180	66	952	2790	0.142	1.37 (1.20-1.58)	7.59 x 10⁻⁶	
	Combined[e]											1.46 (1.28-1.62)	9.15 x 10⁻¹¹	0.075
rs3817963														
	GWAS	a/g	BTNL2 (6p21.3)	92	343	241	0.390	101	437	505	0.306	1.53 (1.29-1.81)	9.50 x 10⁻⁷	
	Replication			130	395	395	0.356	409	1573	1816	0.315	1.22 (1.10-1.36)	2.66 x 10⁻⁴	
	Combined[e]											1.30 (1.18-1.42)	1.28 x 10⁻⁸	0.029
rs9405098														
	GWAS	a/g	No gene (6p21.3)	75	293	308	0.328	70	365	608	0.242	1.54 (1.30-1.84)	1.10 x 10⁻⁶	
	Replication			100	361	462	0.304	249	1429	2129	0.253	1.30 (1.16-1.46)	5.64 x 10⁻⁶	
	Combined[e]											1.37 (1.23-1.50)	1.04 x 10⁻¹⁰	0.105
rs3135363														
	GWAS	c/t	No gene (6p21.3)	35	258	383	0.757	89	447	507	0.700	1.58 (1.32-1.90)	7.89 x 10⁻⁷	
	Replication			73	322	540	0.750	389	1486	1929	0.702	1.30 (1.16-1.46)	7.94 x 10⁻⁶	
	Combined[e]											1.37 (1.24-1.51)	1.45 x 10⁻¹⁰	0.069
rs3129860														
	GWAS	a/g	No gene (6p21.3)	58	294	324	0.303	57	348	638	0.221	1.55 (1.29-1.82)	6.45 x 10⁻⁶	
	Replication			88	339	507	0.276	208	1341	2246	0.231	1.28 (1.14-1.44)	2.53 x 10⁻⁵	
	Combined[e]											1.36 (1.22-1.49)	1.07 x 10⁻⁹	0.085

1618 (682 in GWAS and 936 in replication) liver cirrhosis and 4854 (1045 in GWAS and 3809 in replication) chronic hepatitis C samples were analyzed.
[a]RAF, risk allele frequency.
[b]OR, odds ratios; CI, confidence interval.
[c]p Values obtained by logistic regression analysis adjusted for age and gender under additive model.
[d]p Values of heterogeneities (Phet) across three stages were examined by using the Breslow–Day test.
[e]Combined odds ratio and p values for independence test were calculated by Mendel-hauzen and Laird method in the meta-analysis.

Supplementary Fig. 3). To further evaluate the effect of each variation on the progression from CHC to LC, we performed multiple logistic regression analyses. As a result, rs910049 (p of 1.91 x 10⁻³ with OR of 1.25) and rs3135363 (p of 1.49 x 10⁻⁴ with OR of 1.23) remained significantly associated with the progression risk from CHC to LC, while the remaining three SNPs failed to show significant associations (p >0.05) (Supplementary Table 3). Thus, two SNPs, rs910049 and rs3135363, seem to be independent risk factors for HCV-induced LC.

Since reduced platelet level is associated with a poor prognosis among CHC patients [44] we excluded patients with platelet level of less than 160,000 from CHC groups to increase the risk of type 2 error in this study. We also conducted the analysis using only CHC patients diagnosed with liver biopsy. As a result, both SNPs reached genome-wide significance (p <5 x 10⁻⁸), although the associations were reduced due to the smaller sample size (Supplementary Table 4).

Subgroup analyses, stratified by IFN treatment status, amount of alcohol consumption, and gender, were also performed, since these factors were shown to be associated with the prognosis of CHC patients [45–47]. A total of 334 LC patients (35.83%) and 2325 CHC (82.4%) were treated with IFN therapy. Although the frequency of IFN treatment was different between CHC and LC groups, these variations associated with the LC risk regardless of IFN treatment as well as gender and alcohol consumption (Supplementary Fig. 4A–C). When we included these factors as covariates, the association of these variations with HCV-induced LC was sustained, with OR of 1.48 and 1.56, and SNP rs3135363

still reached genome-wide significance (p = 3.95 x 10⁻⁹) (Supplementary Table 5).

The association of previously reported variations with HCV-induced LC

Non-synonymous SNP rs738409 (I148M) in the *PNPLA3* gene was shown to be associated with progression of LC in the previous prospective study in Caucasians [31]. SNP rs738409 was also associated with the severity of non-alcoholic fatty liver disease in Japanese [48]. Therefore, we analyzed SNP rs738409 in our case-control cohort, but rs738409 did not significantly associate with HCV-induced LC (p = 0.24 and OR = 1.10), although the risk G allele was more frequent among LC than CHC (Supplementary Table 6). Our result is similar to what observed among Caucasians in the previous study, in which rs738409 increased liver cancer risk among alcoholic cirrhosis but did not among hepatitis C cirrhosis [49]. Since biological studies demonstrated that its risk allele (G) abolishes the triglyceride hydrolysis activity of *PNPLA3* [50] *PNPLA3* variation would have a strong impact on non-viral cirrhosis.

Recently, GWAS in the Caucasian population identified the association of SNPs rs4374383, rs16851720 and rs9380516 with the progression of liver fibrosis after HCV infection [51]. However, SNPs rs4374383 and rs16851720 did not exhibit significant association (p = 0.654 and 0.231, respectively) in our sample set. Although SNP rs9380516 exhibited the association with p-value of 0.015, the risk allele showed an opposite result

Table 3. Results of three associated variations from candidate gene analyses.

Gene	Tagging SNP	Haplotype frequency		OR (95% CI)[a]		p value[b]
		Liver cirrhosis	Chronic hepatitis C			
DQA1*0601	rs2736182(T) + rs2071293(A)	0.038	0.019	2.80	1.38-3.32	4.53 x 10⁻⁴
DRB1*0405	rs411326(C) + rs2395185(A) + rs4599680(A)	0.324	0.266	1.45	1.15-1.56	1.54 x 10⁻⁴

Association was tested by comparing haplotype distribution between 682 liver cirrhosis and 1045 chronic hepatitis C samples in GWAS.
[a]OR, odds ratio; CI, confidence interval.
[b]p Values were obtained by case-control analysis of GWAS stage (p for haplotype were obtained by score test, implemented in R) (DQA1*0601 and DRB1*0405). The p values obtained by logistic regression analysis adjusted for age and gender under additive model.

(Supplementary Table 6). Taken together, these SNPs would not be associated with liver fibrosis in the Japanese population.

Genes related to extracellular matrix turnover or immune response (KRT 19, COL1A1, STMN2, CXCL6, CCR2, TIMP1, IL8, IL1A, ITGA2, CLDN 4, and IL2) were shown to be implicated in liver fibrosis of chronic hepatitis C [14]. To further characterize these loci, we conducted imputation analyses in the GWAS sample set (682 cases and 1045 controls), using data from HAPMAP phase II (JPT), and found 163 SNPs in 9 loci. However, none of these SNPs indicated significant association with p-value of less than 0.01 (Supplementary Table 7). Thus, variations of these genes did not associate with progression from chronic hepatitis C to liver cirrhosis.

Imputation-based fine mapping of HLA region

The most significantly associated SNP rs3135363 is located within an intergenic region between BTNL2 and HLA-DRA, and rs910049 is located in intron 7 of C6orf10 gene (Supplementary Figs. 5 and 6). To further characterize these loci, we conducted imputation-based association analysis for the GWAS samples (682 LC and 1045 CHC samples) using data from HAPMAP Phase II (JPT), and could obtain the results of nearly 6000 SNPs in a 4-Mb genomic region. The regional association plots revealed that all modestly-associated SNPs are confined within a 700-kb region containing 21 genes, namely TNXB, ATF6B, FKBPL, PRRT1, PPT2, EGFL8, AGPAT1, RNF5, RNF5P1, AGER, PBX2, C6orf10, BTNL2, HLA-DRA, HLA-DRB5, HLA-DRB6, HLA-DRB1, HLA-DQA1, HLA-DQA2, HLA-DQB1 and HLA-DQB2 (Supplementary Fig. 5). Although 640 SNPs, including ten non-synonymous SNPs within the 4-Mb region, showed very modest associations (p <0.01) with HCV-induced LC, none of these SNPs in this region revealed strong association with HCV-induced LC, after adjustment with the two SNPs, rs910049 and rs3135363 (Supplementary Fig. 7). Taken together, the associations observed in this region would reflect the association with rs910049 and rs3135363.

Previous reports indicated the association of HLA-DRB1 and HLA-DQ alleles with HCV-induced chronic hepatitis in the Japanese population [26]. To investigate the association of HLA alleles with HCV-induced LC, we estimated the genotypes at the HLA region by applying the imputation results of HLA-tagging SNPs [37]. We could successfully determine 53 alleles of HLA-A, B, C, DQA, DQB, and DRB genes and find that HLA-DQA1*0601 and HLA-DRB1*0405 were strongly associated with HCV-induced LC (p values of 4.53 × 10⁻⁴ and 1.54 × 10⁻⁴ with ORs of 2.80 and 1.45) even after the Bonferroni correction (p <0.05/ 53 = 9.43 × 10⁻⁴) (Table 3 and Supplementary Table 8A–E) [37].
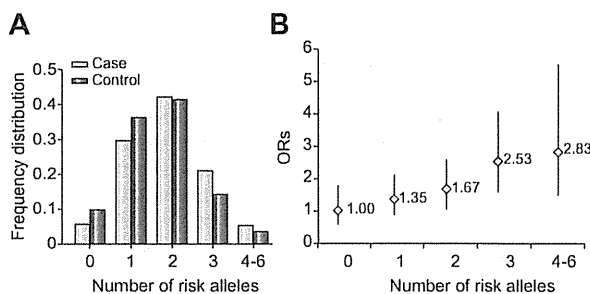

Fig. 2. Cumulative effects of liver cirrhosis risk alleles. (A) Frequency distribution divided by risk allele numbers (rs910049, rs3135353, and HLA-DQA0601) among liver cirrhosis (light blue bars) and chronic hepatitis C (dark blue bars) patients. (B) Plot of the increase odds ratio (OR) for liver cirrhosis according to the number of risk alleles. The ORs are relative to the subjects with no risk alleles (rs910049, rs3135353, and HLA-DQA0601). Vertical bars correspond to 95% confidence intervals. Horizontal line marks the null value (OR = 1).

Cumulative effect of multiple loci within the HLA region

SNPs rs3135363 and rs910049, HLA-DQA1*0601, and HLA-DRB1*0405 are located within a 300-kb segment in the HLA class II region and show moderate linkage disequilibrium (Supplementary Fig. 8). To further evaluate these genetic factors, we performed multiple logistic regression analyses and found that rs910049 (p of 9.40 × 10⁻³ with OR of 1.38), rs3135363 (p of 3.94 × 10⁻⁴ with OR = 1.41), and HLA-DQA1*0601 (p of 7.79 × 10⁻³ with OR of 1.54) were significantly associated with HCV-induced LC (Supplementary Table 9), indicating these three variations were independent risk factors for progression of CHC to LC.

To investigate the pathophysiological roles of rs910049 and rs3135363 in disease progression, we searched the eQTL database (http://www.sph.umich.edu/csg/liang/imputation) and found that risk alleles of rs910049 (A) and rs3135363 (T) were associated with lower expression of HLA-DQA (LOD of ≥6.86 and 17.31, respectively) and DRB1 (LOD of ≥12.01 and 18.96, respectively), and with higher expression of HLA-DQB1 (LOD of ≥6.76 and 4.46, respectively) (Supplementary Table 10). Thus, rs910049 and rs3135363 are likely to affect the expression of HLA class II molecules and subsequently alter the risk of HCV-induced LC.

Finally, we examined the cumulative effects of rs910049, rs3135363, and HLA-DQA1*0601. Individuals with four or more risk alleles (8.8% of general population) have 2.83-fold higher risk of HCV-induced LC compared with those with no risk allele (15.0% of general population, Fig. 2).

Research Article

Discussion

We here demonstrated that multiple genetic variations in the MHC region were significantly associated with the risk of disease progression from CHC to LC, using a total of 1618 HCV-LC and 4854 CHC cases. Since a substantial proportion of patients with CHC show progression to LC in a certain time period, exclusion of CHC patients who have a high risk for LC from control subjects is essential to reduce the risk of false negative association. In this study, CHC patients with advanced fibrosis (F3 or F4 in stage) or with reduced platelet level (less than 160,000/μl) were excluded from the control samples, since these alterations are well-known risk factors for LC development [9,32]. Consequently, we were successfully able to identify the HCV-induced LC loci.

HLA genes are known to play critical roles in the regulation of our immune responses through controlling the antigen presentation to CD8 (class I) and CD4 (class II) T cells. Although previous studies indicated the association of HLA class I alleles such as *HLA-B57*, *HLA-A11*, and *HLA-C04* with persistent HCV infection [52,53], no SNPs in the HLA class I region exhibited strong association with HCV-induced LC. Here we identified three variations (rs910049, rs3135363, *HLA-DQA1*0601*) in the HLA class II region to be significantly associated with the progression risk from CHC to LC. Since two SNPs, rs910049 and rs3135363, had been indicated to affect expression levels of *HLA-DRB1* and *DQ*, our findings indicated the significant pathophysiological roles of HLA class II molecules in the development of HCV-induced liver fibrosis. Considering the function of *HLA-DQ* and *HLA-DR*, we suggest that the antigen presentation by HLA class II molecules is likely to play a critical role in the elimination of HCV-infected liver cells and subsequently prevent HCV-induced LC.

Direct acting antiviral drugs for HCV can cure up to 75% of patients infected with HCV genotype 1, and the lifetime risk of developing LC and HCC among HCV carriers was decreased during the two recent decades [54,13]. However, the amino acid sequence of the NS3 protease domain varies significantly between HCV genotypes and the antiviral efficacy differs in different HCV genotypes [55]. Moreover, protease inhibitors increased the incidence of adverse reactions such as anemia and skin rash [56]. Therefore, estimation of liver cirrhosis risk and prediction of treatment response would be essential to provide a personalized treatment and to achieve the optimal results. Due to the recent advances in pharmacogenetic studies, genetic factors associated with efficacy and adverse effects of anti-HCV treatment were identified. *IL-28B* is a powerful predictor of treatment outcome of pegylated interferon and ribavirin therapy [22], while a genetic variation in the *ITPA* gene was shown to be associated with ribavirin-induced anemia [57]. Since we conducted a retrospective study, and the majority of LC patients did not receive IFN treatment, we could not evaluate the treatment responses in our study design. However, SNPs identified in this study were associated with the LC risk independent of IFN treatment. Although the impact of each SNP was relatively weak compared with viral factors (HCV genotype, core and NS5A mutation [58]) and host factors (age, gender, obesity, and insulin resistance), we found that individuals with three or more risk alleles have a nearly three-fold higher risk of LC than those with no risk allele. Since lifetime risk of HCC development among HCV carriers is as high as about 27% for male and 8% for female [59], these three loci would have the strong effect on the clinical outcome of CHC patients. In general, the progression from chronic hepatitis C to liver cirrhosis usually takes more than 20–30 years. Therefore,

a large scale prospective cohort study with more than 10-year follow-up is essential to evaluate the role of these variations as a prognostic biomarker. We would like to perform prospective analysis in future studies. We hope that our findings would contribute to clarify the underling molecular mechanism of HCV-induced liver cirrhosis.

Conflict of interest

The authors who have taken part in this study declared that they do not have anything to disclose regarding funding or conflict of interest with respect to this manuscript.

Authors' contributions

Y. U., K. K., K. C., and K.M. conceived and designed the study; Y. U., H. O., N. K., Y. K., R. M., N. H., and M. K. performed genotyping; A. T., P. H. Y. L., C. T., and N. K. performed quality control at genome-wide phase; M. O., R. T., M. O., K. K., D. M., H. A., J. T., H. K., Y. N., K. M. and M. K. managed DNA samples; Y. U. analyzed and summarized the whole results; Y. U., Y. N., and K. M. wrote the manuscript; Y. N. obtained funding for the study.

Supplementary data

Supplementary data associated with this article can be found, in the online version, at http://dx.doi.org/10.1016/j.jhep.2012.12.024.

References

[1] Shepard CW, Finelli L, Alter MJ. Global epidemiology of hepatitis C virus infection. Lancet Infect Dis 2005;5:558–567.
[2] Seeff LB. Natural history of chronic hepatitis C. Hepatology 2002;36:S35–S46.
[3] Thomas DL, Seeff LB. Natural history of hepatitis C. Clin Liver Dis 2005;9:383–398, vi.
[4] Freeman AJ, Dore GJ, Law MG, Thorpe M, Von Overbeck J, Lloyd AR, et al. Estimating progression to cirrhosis in chronic hepatitis C virus infection. Hepatology 2001;34:809–816.
[5] Hoofnagle JH. Hepatitis C: the clinical spectrum of disease. Hepatology 1997;26:15S–20S.
[6] Tanaka H, Imai Y, Hiramatsu N, Ito Y, Imanaka K, Oshita M, et al. Declining incidence of hepatocellular carcinoma in Osaka, Japan, from 1990 to 2003. Ann Intern Med 2008;148:820–826.

[7] Global burden of disease (GBD) for hepatitis C. J Clin Pharmacol 2004;44:20–29.

[8] Poynard T, Bedossa P, Opolon P. Natural history of liver fibrosis progression in patients with chronic hepatitis C. The OBSVIRC, METAVIR, CLINIVIR, and DOSVIRC groups. Lancet 1997;349:825–832.

[9] Yoshida H, Shiratori Y, Moriyama M, Arakawa Y, Ide T, Sata M, et al. Interferon therapy reduces the risk for hepatocellular carcinoma: national surveillance program of cirrhotic and noncirrhotic patients with chronic hepatitis C in Japan. IHIT Study Group. Inhibition of hepatocarcinogenesis by interferon therapy. Ann Intern Med 1999;131:174–181.

[10] Zhang Q, Tanaka K, Sun P, Nakata M, Yamamoto R, Sakimura K, et al. Suppression of synaptic plasticity by cerebrospinal fluid from anti-NMDA receptor encephalitis patients. Neurobiol Dis 2012;45:610–615.

[11] Aghemo A, Prati GM, Rumi MG, Soffredini R, D'Ambrosio R, Orsi E, et al. A sustained virological response prevents development of insulin resistance in chronic hepatitis C patients. Hepatology 2012;56:549–556.

[12] Bièche I, Asselah T, Laurendeau I, Vidaud D, Degot C, Paradis V, et al. Molecular profiling of early stage liver fibrosis in patients with chronic hepatitis C virus infection. Virology 2005;332:130–144.

[13] Estrabaud E, Vidaud M, Marcellin P, Asselah T. Genomics and HCV infection: progression of fibrosis and treatment response. J Hepatol 2012;57:1110–1125.

[14] Asselah T, Bièche I, Laurendeau I, Paradis V, Vidaud D, Degott C, et al. Liver gene expression signature of mild fibrosis in patients with chronic hepatitis C. Gastroenterology 2005;129:2064–2075.

[15] Marquez RT, Bandyopadhyay S, Wendlandt EB, Keck K, Hoffer BA, Icardi MS, et al. Correlation between microRNA expression levels and clinical parameters associated with chronic hepatitis C viral infection in humans. Lab Invest 2010;90:1727–1736.

[16] Morita K, Taketomi A, Shirabe K, Umeda K, Kayashima H, Ninomiya M, et al. Clinical significance and potential of hepatic microRNA-122 expression in hepatitis C. Liver Int 2011;31:474–484.

[17] Cui R, Okada Y, Jang SG, Ku JL, Park JG, Kamatani Y, et al. Common variant in 6q26-q27 is associated with distal colon cancer in an Asian population. Gut 2011;60:799–805.

[18] Kumar V, Matsuo K, Takahashi A, Hosono N, Tsunoda T, Kamatani N, et al. Common variants on 14q32 and 13q12 are associated with DLBCL susceptibility. J Hum Genet 2011;56:436–439.

[19] Tanikawa C, Urabe Y, Matsuo K, Kubo M, Takahashi A, Ito H, et al. A genome-wide association study identifies two susceptibility loci for duodenal ulcer in the Japanese population. Nat Genet 2012;44:430–434.

[20] Urabe Y, Tanikawa C, Takahashi A, Okada Y, Morizono T, Tsunoda T, et al. A genome-wide association study of nephrolithiasis in the Japanese population identifies novel susceptible loci at 5q35.3, 7p14.3, and 13q14.1. PLoS Genet 2012;8:e1002541.

[21] Thomas DL, Thio CL, Martin MP, Qi Y, Ge D, O'Huigin C, et al. Genetic variation in IL28B and spontaneous clearance of hepatitis C virus. Nature 2009;461:798–801.

[22] Tanaka Y, Nishida N, Sugiyama M, Kurosaki M, Matsuura K, Sakamoto N, et al. Genome-wide association of IL28B with response to pegylated interferon-alpha and ribavirin therapy for chronic hepatitis C. Nat Genet 2009;41:1105–1109.

[23] Suppiah V, Moldovan M, Ahlenstiel G, Berg T, Weltman M, Abate ML, et al. IL28B is associated with response to chronic hepatitis C interferon-alpha and ribavirin therapy. Nat Genet 2009;41:1100–1104.

[24] Kumar V, Kato N, Urabe Y, Takahashi A, Muroyama R, Hosono N, et al. Genome-wide association study identifies a susceptibility locus for HCV-induced hepatocellular carcinoma. Nat Genet 2011;43:455–458.

[25] Miki D, Ochi H, Hayes CN, Abe H, Yoshima T, Aikata H, et al. Variation in the DEPDC5 locus is associated with progression to hepatocellular carcinoma in chronic hepatitis C virus carriers. Nat Genet 2011;43:797–800.

[26] Kuzushita N, Hayashi N, Moribe T, Katayama K, Kanto T, Nakatani S, et al. Influence of HLA haplotypes on the clinical courses of individuals infected with hepatitis C virus. Hepatology 1998;27:240–244.

[27] Singh R, Kaul R, Kaul A, Khan K. A comparative review of HLA associations with hepatitis B and C viral infections across global populations. World J Gastroenterol 2007;13:1770–1787.

[28] Mosaad YM, Farag RE, Arafa MM, Eletreby S, El-Alfy HA, Eldeek BS, et al. Association of human leucocyte antigen Class I (HLA-A and HLA-B) with chronic hepatitis C virus infection in Egyptian patients. Scand J Immunol 2010;72:548–553.

[29] Li CZ, Kato N, Chang JH, Muroyama R, Shao RX, Dharel N, et al. Polymorphism of OAS-1 determines liver fibrosis progression in hepatitis C by reduced ability to inhibit viral replication. Liver Int 2009;29:1413–1421.

[30] Mozer-Lisewska I, Sikora J, Kowala-Piaskowska A, Kaczmarek M, Dworacki G, Zeromski J. The incidence and significance of pattern-recognition receptors in chronic viral hepatitis types B and C in man. Arch Immunol Ther Exp (Warsz) 2010;58:295–302.

[31] Trépo E, Pradat P, Potthoff A, Momozawa Y, Quertinmont E, Gustot T, et al. Impact of patatin-like phospholipase-3 (rs738409 C>G) polymorphism on fibrosis progression and steatosis in chronic hepatitis C. Hepatology 2011;54:60–69.

[32] Romero-Gómez M, Gómez-González E, Madrazo A, Vera-Valencia M, Rodrigo L, Pérez-Alvarez R, et al. Optical analysis of computed tomography images of the liver predicts fibrosis stage and distribution in chronic hepatitis C. Hepatology 2008;47:810–816.

[33] Nakamura Y. The BioBank Japan project. Clin Adv Hematol Oncol 2007;5:696–697.

[34] Purcell S, Neale B, Todd-Brown K, Thomas L, Ferreira M, Bender D, et al. PLINK: a tool set for whole-genome association and population-based linkage analyses. Am J Hum Genet 2007;81:559–575.

[35] Frazer KA, Ballinger DG, Cox DR, Hinds DA, Stuve LL, Gibbs RA, et al. A second generation human haplotype map of over 3.1 million SNPs. Nature 2007;449:851–861.

[36] Breslow NE, Day NE. Statistical methods in cancer research. The design and analysis of cohort studies. IARC Sci Publ 1987;II:1–406.

[37] de Bakker PI, McVean G, Sabeti PC, Miretti MM, Green T, Marchini J, et al. A high-resolution HLA and SNP haplotype map for disease association studies in the extended human MHC. Nat Genet 2006;38:1166–1172.

[38] Scott LJ, Mohlke KL, Bonnycastle LL, Willer CJ, Li Y, Duren WL, et al. A genome-wide association study of type 2 diabetes in Finns detects multiple susceptibility variants. Science 2007;316:1341–1345.

[39] Consortium GP. A map of human genome variation from population-scale sequencing. Nature 2010;467:1061–1073.

[40] Barrett J, Fry B, Maller J, Daly M. Haploview: analysis and visualization of LD and haplotype maps. Bioinformatics 2005;21:263–265.

[41] Xu Z, Taylor JA. SNPinfo: integrating GWAS and candidate gene information into functional SNP selection for genetic association studies. Nucleic Acids Res 2009;37:W600–W605.

[42] Dixon AL, Liang L, Moffatt MF, Chen W, Heath S, Wong KC, et al. A genome-wide association study of global gene expression. Nat Genet 2007;39:1202–1207.

[43] Kel AE, Gössling E, Reuter I, Cheremushkin E, Kel-Margoulis OV, Wingender E. MATCH: a tool for searching transcription factor binding sites in DNA sequences. Nucleic Acids Res 2003;31:3576–3579.

[44] Wai CT, Greenson JK, Fontana RJ, Kalbfleisch JD, Marrero JA, Conjeevaram HS, et al. A simple noninvasive index can predict both significant fibrosis and cirrhosis in patients with chronic hepatitis C. Hepatology 2003;38:518–526.

[45] Cammà C, Di Bona D, Schepis F, Heathcote EJ, Zeuzem S, Pockros PJ, et al. Effect of peginterferon alfa-2a on liver histology in chronic hepatitis C: a meta-analysis of individual patient data. Hepatology 2004;39:333–342.

[46] Marcellin P, Asselah T, Boyer N. Fibrosis and disease progression in hepatitis C. Hepatology 2002;36:S47–S56.

[47] Silini E, Bottelli R, Asti M, Bruno S, Candusso ME, Brambilla S, et al. Hepatitis C virus genotypes and risk of hepatocellular carcinoma in cirrhosis: a case-control study. Gastroenterology 1996;111:199–205.

[48] Kawaguchi T, Sumida Y, Umemura A, Matsuo K, Takahashi M, Takamura T, et al. Genetic polymorphisms of the human PNPLA3 gene are strongly associated with severity of non-alcoholic fatty liver disease in Japanese. PLoS One 2012;7:e38322.

[49] Nischalke HD, Berger C, Luda C, Berg T, Müller T, Grünhage F, et al. The PNPLA3 rs738409 148M/M genotype is a risk factor for liver cancer in alcoholic cirrhosis but shows no or weak association in hepatitis C cirrhosis. PLoS One 2011;6:e27087.

[50] He S, McPhaul C, Li JZ, Garuti R, Kinch L, Grishin NV, et al. A sequence variation (I148M) in PNPLA3 associated with nonalcoholic fatty liver disease disrupts triglyceride hydrolysis. J Biol Chem 2010;285:6706.

[51] Patin E, Kutalik Z, Guergnon J, Bibert S, Nalpas B, Jouanguy E, et al. Genome-wide association study identifies variants associated with progression of liver fibrosis from HCV infection. Gastroenterology 2012;143: 124–152, e1–12.

[52] Kim AY, Kuntzen T, Timm J, Nolan BE, Baca MA, Reyor LL, et al. Spontaneous control of HCV is associated with expression of HLA-B 57 and preservation of targeted epitopes. Gastroenterology 2011;140:e681.

[53] Fanning LJ, Kenny-Walsh E, Shanahan F. Persistence of hepatitis C virus in a white population: associations with human leukocyte antigen class 1. Hum Immunol 2004;65:745–751.

198

Research Article

[54] Imhof I, Simmonds P. Genotype differences in susceptibility and resistance development of hepatitis C virus to protease inhibitors telaprevir (VX-950) and danoprevir (ITMN-191). Hepatology 2011;53:1090–1099.

[55] Asselah T, Marcellin P. Direct acting antivirals for the treatment of chronic hepatitis C: one pill a day for tomorrow. Liver Int 2012;32: 88–102.

[56] Ozeki I, Akaike J, Karino Y, Arakawa T, Kuwata Y, Ohmura T, et al. Antiviral effects of peginterferon alpha-2b and ribavirin following 24-week mono-therapy of telaprevir in Japanese hepatitis C patients. J Gastroenterol 2011;46:929–937.

[57] Ochi H, Maekawa T, Abe H, Hayashida Y, Nakano R, Kubo M, et al. ITPA polymorphism affects ribavirin-induced anemia and outcomes of therapy –

a genome-wide study of Japanese HCV virus patients. Gastroenterology 2010;139:1190–1197.

[58] Enomoto N, Sakuma I, Asahina Y, Kurosaki M, Murakami T, Yamamoto C, et al. Mutations in the nonstructural protein 5A gene and response to interferon in patients with chronic hepatitis C virus 1b infection. N Engl J Med 1996;334:77–82.

[59] Huang YT, Jen CL, Yang HI, Lee MH, Su J, Lu SN, et al. Lifetime risk and sex difference of hepatocellular carcinoma among patients with chronic hepatitis B and C. J Clin Oncol 2011;29:3643–3650.

199